

## Chapter 2

# Orifice Design

**Abstract** This chapter describes the main design specifications for orifice plates (more precisely, orifice meters): it points the reader to important parts of ISO 5167 and gives reasons for the requirements in the standard. It covers the orifice plate (the circularity of the bore, the flatness, the parallelism of the two faces, the surface condition of the upstream face, and, above all, the edge sharpness), the pipe (the pressure tapings, the pipe roughness, the effect of upstream steps, the concentricity of the orifice plate in the pipe and the circularity and cylindricity of the pipe), the measurements of both the orifice plate and the pipe, and the pressure loss. A very significant incorrect installation of an orifice plate within the pipe, a reversed orifice plate, is also covered. Appendix 2.A considers the use of orifice plates of diameter smaller than that permitted in ISO 5167. The effect of upstream fittings is not covered here: it is Chap. 8. The basic instruction remains to follow ISO 5167. For some important deviations from ISO 5167 the errors in discharge coefficient can be calculated using what is described in this chapter.

### 2.1 Introduction

An orifice plate is fundamentally a plate with a hole machined through it which is inserted into a pipe. As flow passes through the hole it produces a pressure difference across the hole (some of which is recovered). The plate must be sufficiently thin that over the range of permitted thickness its thickness does not affect the discharge coefficient but thick enough not to be distorted by the forces imposed by the pressure difference. The pressure difference is proportional to the square of the flowrate (mass or volume).

The hole may be of any shape if the discharge coefficient is determined by calibration. A few shapes and designs have been produced for which the discharge coefficient can be predicted. Of these only for a round sharp-edged centrally located hole are there sufficient data to allow prediction of flowrate with an uncertainty which is low enough to use for trade in the most valuable fluids: only this shape is covered in this book. Other shapes are listed in NOTE 1 of Chap. 1.

The main design specifications are in ISO 5167-1:2003 and ISO 5167-2:2003 (ISO 2003a, b). This chapter points the reader to important parts of ISO 5167 and gives reasons for the requirements in the standard. It covers the orifice plate (the circularity of the bore, the flatness, the parallelism of the two faces, the surface condition of the upstream face, and, above all, the edge sharpness), the pipe (the pressure tapings, the pipe roughness, the effect of upstream steps, the concentricity of the orifice plate in the pipe and the circularity and cylindricity of the pipe), the measurements of both the orifice plate and the pipe, and the pressure loss. A very significant incorrect installation of an orifice plate within the pipe, a reversed orifice plate, is also covered. Appendix 2.A considers the use of orifice plates of diameter smaller than that permitted in ISO 5167-2:2003. The installation of the orifice meter (the orifice plate and pipe) in terms of upstream straight lengths, flow conditioners and pulsations is covered in Chap. 8.

To design an orifice plate, given the range of mass flowrates, the density, the desired range of differential pressures (discussed in Sect. 4.3), the discharge coefficient (from Chap. 5), the expansibility factor (from Chap. 6) and the desired pipe diameter ( $D$ ), the throat diameter ( $d$ ) can be determined from Eq. 1.15:

$$q_m = \frac{C_\varepsilon}{\sqrt{1 - \beta^4}} \frac{\pi d^2}{4} \sqrt{2\rho_1 \Delta p}. \quad (1.15)$$

If this gives too large a value of diameter ratio ( $\beta$ ) ( $=d/D$ ) then a larger value of  $D$  is required (or a second orifice meter in parallel could be used). For best accuracy  $0.2 \leq \beta \leq 0.6$  is recommended. The uncertainty increases if  $\beta$  is outside this range. If there is no preferred value of  $D$  then it would be good to choose a value of  $D$  so that  $0.5 \leq \beta \leq 0.6$ . As  $\beta$  increases the effects of pipe roughness (see Sect. 2.3.3), installation (see Chap. 8) and eccentricity (see Sect. 2.3.5) increase: this is reflected in an increase in the uncertainty of the discharge-coefficient equation (see 5.3.3.1 of ISO 5167-2:2003 and Fig. 5.12). As  $\beta$  is reduced the pressure loss increases. If  $\beta < 0.2$  there is a scarcity of data (see Chap. 5) and unless  $D$  is large there are increasing problems with edge sharpness (see Sect. 2.2.4); there is an increase in the uncertainty of the discharge coefficient.

## 2.2 Orifice Plate

### 2.2.1 General

The orifice plate is as in Fig. 2.1 (see also Fig. 2.2: the plate pictured is for insertion between flanges and has a handle for ease of removal). Good quality of manufacture is very important, especially the following:

- The circularity of the bore (5.1.8.3 of ISO 5167-2:2003) (see Sect. 2.4)
- the flatness (5.1.3.1 of ISO 5167-2:2003; see Sect. 2.2.2),

**Fig. 2.1** Orifice plate nomenclature

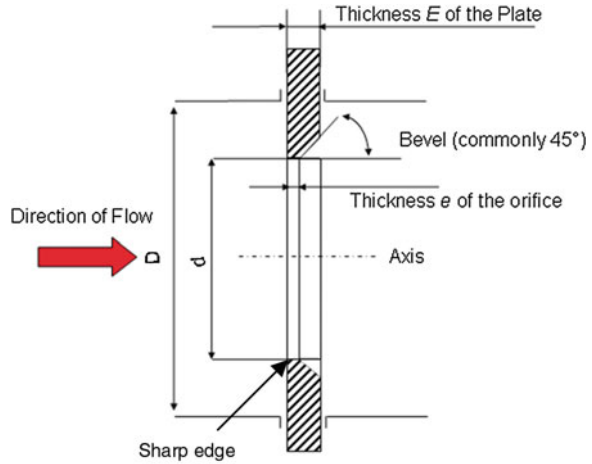


**Fig. 2.2** An orifice plate



- the parallelism of the two faces (5.1.5.4 of ISO 5167-2:2003),
- the surface condition of the upstream face (5.1.3.2 of ISO 5167-2:2003; see Sect. 2.2.3),
- and, above all, the edge sharpness (5.1.7.2 of ISO 5167-2:2003; see Sect. 2.2.4).

The requirement for parallelism is not, as far as the author knows, based on experiment, but simply on what can reasonably be manufactured; that is why there are different requirements for  $D < 200$  mm. This lack of similarity suggests that the requirement for larger orifice plates may be sufficient but not necessary. The required values for the thicknesses of the orifice plate ( $E$ ) and of the orifice bore ( $e$ ) are based on experiment (see Sect. 2.2.5).

## 2.2.2 Flatness

The effect of buckling an orifice plate was measured by Jepson and Chipchase (1973, 1975) who measured the effect of bending  $\beta = 0.2$  and  $\beta = 0.7$  plates in an 8" line. The deflections of the orifice bore were in the range  $0.0039D$  to  $0.0625D$  [0.79 to 12.7 mm ( $1/32"$  to  $1/2"$ )]. An under-estimation of flow of up to 14 % was measured. The experimental work was compared with theoretical work in which the effects of changing the bore position relative to the pressure tapings, of changing the inward radial momentum of the fluid and of changing the bore size were considered. The first was shown to be smaller than the other two and was neglected. Quite good agreement between experiment and theory was obtained. Work was also undertaken by Gorter (1978). Ting (1993) reported results with 4" and 6" orifice plates that had been bent by a press, and his results were compared with the theory of Mason et al. (1975). The data are presented in Fig. 2.3. With a slope of 1 % the theoretical model of Jepson and Chipchase shown gives a shift in discharge coefficient of a little less than 0.2 % in absolute value at maximum.

The fundamental need is that the orifice plate not be bent in such a way as to cause a significant shift in discharge coefficient. It can be bent both by poor manufacture and by the effect of the differential pressure across it. The former can be measured in the laboratory; the latter (except in the case of permanent distortion) cannot. It must be calculated. The requirement on which ISO 5167-2:2003 is based is that the discharge coefficient should not change by more than 0.2 % from the value given by a flat plate perpendicular to the pipe axis (Norman et al. 1983). This corresponds to a requirement that the plate should not have a slope ( $=2\delta/(D - d)$ ) greater than 1 % (this assumes that the experimental data for  $\beta = 0.2$  in Fig. 2.3 have quite high

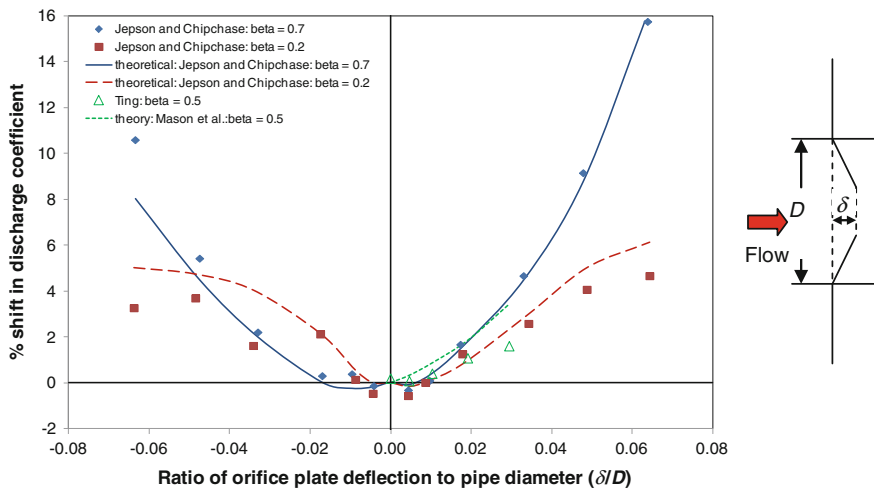


**Fig. 2.3** The effect of bending an orifice plate: positive deflection ( $\delta$ ) is in the downstream direction

uncertainty, but that the theoretical model of Jepson and Chipchase can be used). To ensure this, the slope of the plate should not exceed 0.5 % when measured in the laboratory and the differential pressure should not cause a slope of more than 0.5 %. The slope in the laboratory can be measured using feeler gauges. Advice on how to calculate the maximum differential pressure so that the orifice plate is neither elastically deformed beyond the permitted limit nor permanently buckled is given in 5.2.5.1.2.3 of ISO/TR 9464:2008 (ISO 2008). To carry out the calculation the material of the plate, the thickness and how it is supported at the outside edge must be known. More accurate predictions can be calculated using finite element analysis; however, ISO/TR 9464 will normally provide adequate guidance.

### 2.2.3 Surface Condition of the Upstream Face of the Plate

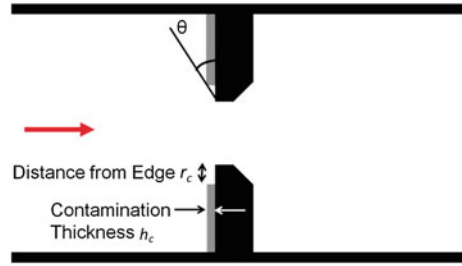
The requirement (in 5.1.3.2 of ISO 5167-2:2003) on the roughness of the upstream face of the orifice plate that  $R_a < 10^{-4}d$  is normally fairly easy to meet at manufacture (definitions of  $R_a$  and  $k$  are given in Sect. 2.3.3.1). If it were exceeded it would make it difficult to meet the edge-sharpness requirement. It appears to be based on work of McVeigh (1962) and Dall (1958); McVeigh recommends that  $k/d \leq 3 \times 10^{-4}$ , which is equivalent to the ISO limit: some of McVeigh's data were taken in a 1" pipe. Data were taken by Studzinski and Berg (1988), but these are surprising: the effect of  $R_a = 2 \mu\text{m}$  is greater in an 8" pipe than in a 4" pipe. Computational work by Reader-Harris (1991, 1993) concluded that the ISO limit is reasonable for  $Re_d \approx 10^7$  and conservative for smaller  $Re_d$ . 2.4.1 of API MPMS 14.3.2 (API 2000) requires a maximum of 1.27  $\mu\text{m}$  (50  $\mu\text{in.}$ ); this is sufficient (but not non-dimensional); the plates used by API to provide data used to develop the orifice discharge-coefficient equation had  $R_a$  in the range 0.10–0.53  $\mu\text{m}$  (4–21  $\mu\text{in.}$ ).

One important cause of poor surface condition in practice is the presence of contamination due to deposition. This is covered in 9.3 of ISO/TR 12767:2007 (ISO 2007c), which contains some examples of the effect of contamination (Pritchard et al. 2003, 2004), but does not give a general formula for its effect. The experiments by Pritchard et al. used grease on an orifice plate; this grease moved during the test. Experiments on the effect of grease deposits on an orifice plate have also been performed by Botros et al. (1992) and by Burgin (1971).

The importance of the final portion of the orifice plate approaching the sharp edge can be seen from Morrison et al. (1990): the pressure on the front face of the orifice changes very slowly near the corner between the orifice plate and the pipe, but very rapidly over the portion of the face between a circle whose diameter is about  $1.1d$  and the sharp edge.

There are two patterns of contamination that may occur: one is contamination up to the orifice edge, the other contamination in which a clean ring (kept clean by the flow) is left. The first gives an error that is impossible to predict (it can be directly measured), because the contamination changes the edge sharpness and has a potentially very large effect; some examples of shifts in discharge coefficient are

**Fig. 2.4** A contaminated orifice plate



given in Tables 5 and 6 of ISO/TR 12767:2007. The second has been analysed by Reader-Harris et al. (2010); both computational and experimental work were carried out with a uniform layer of contamination of thickness  $h_c$  on the front face of an orifice plate, starting a distance  $r_c$  from the orifice edge, as shown in Fig. 2.4. The key idea of using  $\theta$ , the largest angle between the sharp edge and the contamination, was due to Neil Barton at NEL.

The percentage shift,  $S$ , in discharge coefficient due to contamination of this pattern was shown to be

$$S = 22.8 \left( \frac{h_c}{r_c} \right)^{1.4} \left( 1 - \frac{2r_c}{D(1 - \beta)} \right)^4 \quad (2.1)$$

This has an uncertainty of 0.28 % based on 2 standard deviations (Reader-Harris et al. 2010).

The effect of very small amounts of liquid in a gas flow can be similar to that of contamination (Ting and Corpron 1995).

The effects of oil coating on orifice plates and pipes have been considered by Johansen et al. (1966) and Johansen (1966). Generally coating the pipe has more effect than coating the plate. Moreover, as would be expected, the effect of coating the pipe increases rapidly with  $\beta$  (see also Morrow 1998). The discharge coefficient increases, but the effect generally reduces with time as the flow removes the oil. Botros et al. (1992) found that very thin liquid films reduce surface roughness and thus the discharge coefficient, an effect not seen in Johansen's or Morrow's work.

The condition of the downstream face of the orifice plate is much less important than that of the upstream (Hobbs and Humphreys 1990): when a plate was roughened by sticking sandpaper of particle size about 1 mm to the downstream face of orifice plates of diameter ratio 0.4, 0.6 and 0.75 in a 12" line there was no significant change in discharge coefficient; it did not matter whether the roughness was over the whole of the downstream face or simply on the bevel.

In conclusion, contamination is the main cause of problems with surface condition: the main aim must be to avoid contamination. Where this is not possible, there is one pattern of contamination where the error can be predicted from the contamination adhering to the plate; in other situations the error needs to be directly measured.

### 2.2.4 Edge Sharpness

A rounded orifice upstream edge leads to error because the flow remains attached to the initial part of the rounded edge: therefore there is an increase in the area of the *vena contracta* and thus in the discharge coefficient.

The edge sharpness of an orifice plate may be destroyed by erosion, cavitation or poor handling.

This is a particularly critical area for small orifice plates. To achieve the required sharpness in large plate sizes, i.e.  $d > 100$  mm, is straightforward at manufacture, although subsequent damage is possible. When  $d < 50$  mm it is difficult, and for  $d < 25$  mm very difficult.

The effect of edge radius, i.e. the radius of the sharp edge,  $r$ , is a well-worked area. It is discussed in Hobbs and Humphreys (1990). The effect is given in Fig. 2.5, which shows their data, taken in 12" pipe. The data points with the smallest value of  $r/d$  for each  $\beta$  are taken as having no shift in discharge coefficient. The slope of the fitted line is approximately 550; so the effect of a change of edge radius of  $0.0002d$  on  $C$  is 0.11 %.

Data have also been taken in 2" and 4" pipe (Herning 1962), 6" pipe (Herning and Wolowski 1963), 3" pipe (Crocket and Upp 1973) and 4" pipe (Benedict et al. 1974). These are shown together with the NEL data in Fig. 1 of ISO/TR 12767:2007 (ISO 2007c). Data with  $r/d$  up to 0.025 were taken by Burgin (1971).

The effect of edge sharpness is also discussed in Spencer et al. (1969) (see below).

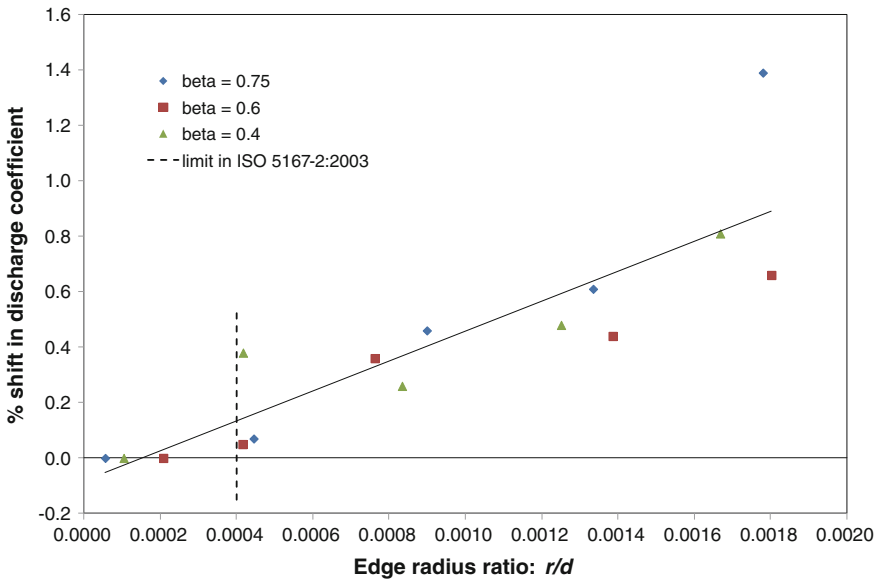


Fig. 2.5 Effect of orifice edge radius ( $r$ ) on discharge coefficient: NEL tests

Measurement techniques for edge radius are available including casting (Gallagher 1968), lead foil impression (Crocket and Upp 1973), and an optical method in which the condition of the orifice edge is determined by observing the distortion caused by a fine beam of light falling onto the edge (Benedict et al. 1974): the results are compared in Brain and Reid (1973).

Measurements of the edge radii of the plates used for the EEC data for the discharge-coefficient equation are given in Spencer (1987): techniques for the same plate included lead foil, casting and profilometry, in which a Talysurf or equivalent machine is used: the typical spread of measurements of the same plate in different laboratories was around  $\pm 5$  to  $\pm 20$   $\mu\text{m}$ , based on the average value of edge radius taken in a laboratory; the spread of measurements at different points of the circumference for a single plate in one laboratory could be as large as  $\pm 20$   $\mu\text{m}$ .

In almost all cases it is better to manufacture the edge sharpness at the required value rather than to attempt to measure it and make appropriate corrections.

From this work comes the requirement that  $r \leq 0.0004d$ , where  $r$  is the radius of the edge. In practice the uncertainty of the measurement tends to be about 10  $\mu\text{m}$  at best. So for small  $d$  it may not be clear whether or not a plate has passed. Difficulties in measurement of edge radius led to difficulty in determining how the plates with small diameters should be used in determining the orifice-plate discharge-coefficient equation. Certainly for  $d$  less than about 38 mm edge radius is a cause of additional uncertainty. The fact that the plates in 3" pipe gave data in agreement with the data for larger sizes is more remarkable than that the plates in 2" pipe did not. It is common to look at an orifice upstream edge and to decide that it is unacceptable if it reflects a beam of light when viewed without magnification. This method enables some poor plates to be identified but takes no account of the fact that the required edge sharpness is proportional to orifice diameter.

One possible solution for small orifices is to spark-erode them. The consequences of using this technique require more research, but it appears that one manufacturer gave a consistent edge radius of about 9  $\mu\text{m}$ . This gives sharp edges for  $d \geq 25$  mm. This area is investigated in Appendix 2.A.

Another source of error is damage to an edge by a chip, nick or groove in the sharp edge. It is helpful to distinguish between a notch that extends completely through the orifice bore (increasing the orifice area) and a groove that cuts the upstream face of the plate and the sharp edge but does not increase the orifice area. The tests of Humphreys and Hobbs (1990) were of the latter type and gave remarkably small effects even where a large amount of damage was inflicted on the plate: for example, a cold chisel was held at an angle of  $45^\circ$  against the sharp edge and struck with a hammer: the metal was not removed but displaced. After one strike the dimensions of the damage were of the order of 2 mm for  $\beta = 0.34$  and 3 mm for  $\beta = 0.75$  in a 12" line: the area of the bore was not increased; the increase in discharge coefficient in the case of both plates was in the range 0.02 or 0.03 to 0.18 % depending on the location of the damage relative to the pressure tappings. A further strike increased the damage to the order of 3 mm for  $\beta = 0.34$  and 4 mm for  $\beta = 0.75$ : then there was a *decrease* in discharge coefficient from that of the undamaged plate of 0.33 % to 0.51 % for  $\beta = 0.34$  and 0.10 % to 0.20 % for



$\beta = 0.75$  depending on the location of the damage relative to the pressure tappings. Botros et al. (1992) undertook a study of the effect of both a groove and a notch. The effect of a notch that extends through the plate is approximately  $\frac{4}{3}$  times the effect of the area increase (and at maximum twice the area increase). Botros et al. state that a typical small nick encountered in a pipeline system causes a measurement error of the order of  $-0.002\%$ .

In conclusion, the sharpness of the upstream edge of the orifice plate is of the utmost importance to the accuracy of the flow measurement. In fiscal measurement systems the orifice plate is checked regularly mainly because of the risk that its edge might be damaged (the check will also find any contamination adhering to the surface). A large defect on a small part of the sharp edge has a small effect on the discharge coefficient, whereas a small defect over the whole of the sharp edge has a large effect.

## 2.2.5 Plate Thickness $E$ and Orifice (Bore) Thickness $e$

### 2.2.5.1 General

Essentially the plate thickness  $E$  has to be sufficiently large that the plate does not bend significantly (see Sect. 2.2.2) but sufficiently small that the installation is geometrically similar to those used for determining the orifice discharge-coefficient equation (Chap. 5). The orifice (bore) thickness  $e$  has to be sufficiently small that the orifice is essentially a thin plate but sufficiently large that a square edge can be obtained. Where  $e < E$  the plate is bevelled.

The plate thickness is easy to measure with a micrometer caliper. Measuring the orifice (bore) thickness using a depth micrometer is less accurate.

### 2.2.5.2 Plate Thickness $E$

Husain and Teyssandier (1986b) measured the shift in discharge coefficient in a 6" flange-tapped orifice meter between a baseline with  $E = 3.2$  mm ( $1/8"$ ) and tests with values of  $E$  up to 19 mm ( $3/4"$ ). Throughout  $e$  was 2.8 mm ( $0.11"$ ). Bevel angles of  $45^\circ$  and  $30^\circ$  (to the pipe axis) were used. To do this the plate was initially 19 mm ( $3/4"$ ) thick and was successively machined thinner. Part of the effect of changing the plate thickness  $E$  is to move downstream corner or flange tappings relative to the upstream face of the plate: the difference in discharge coefficient between an orifice plate of standard thickness with the downstream tapping ( $E - 3.2$  mm) downstream of the flange tapping and the baseline (which is an orifice plate of standard thickness with flange tappings) was calculated from the Reader-Harris/Gallagher (1998) Equation (Eq. 5.22) [5.3.2.1 of ISO 5167-2:2003 (ISO 2003b)]; this is described in Fig. 2.6 as the simple model.

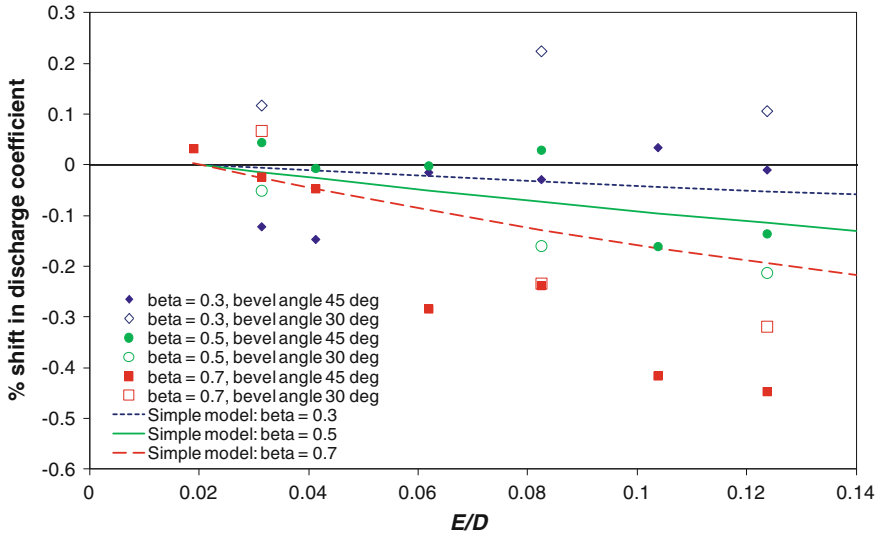


**Fig. 2.6** Effect of changing  $E/D$ . In the simple model the shift is based on the location of the downstream tapping relative to the downstream face of the baseline plate

In Fig. 2.6 the experimental data for  $\beta = 0.3$  are surprisingly scattered; those for  $\beta = 0.5$  are in good agreement with the simple model; those for  $\beta = 0.7$  show a larger shift than the simple model, presumably because in the simple model there is a flow in the part of the orifice meter which in the experiment is the downstream part of the plate.

### 2.2.5.3 Orifice (Bore) Thickness $e$

The effect of increasing the orifice (bore) thickness  $e$  is to change the orifice from a thin orifice, in which it is as if  $e$  were as close as possible to 0 given that a square edge is required on the orifice, to a thick orifice, whose discharge coefficient is around 0.8, because the flow has now reattached to the orifice bore. The discharge coefficient changes slowly where  $e/d$  is small but more rapidly around  $e/d = 0.5$ . This is well exhibited in a set of data from NBS (now NIST) (see Lansverk 1990) given in Fig. 2.7. Flow is unstable where the flow reattaches intermittently to the orifice bore.

In addition to the tests described in Sect. 2.2.5.2, Husain and Teyssandier (1986) measured the shift in discharge coefficient using an unbevelled orifice plate in a 6" flange-tapped orifice meter from a baseline with  $E = e = 3.2$  mm (1/8") to tests with values of  $E$  ( $=e$ ) up to 19 mm (3/4"). To do this the plate was initially 19 mm (3/4") thick and was successively machined thinner. The data are shown in Fig. 2.8.

The famous OSU data (Beitler 1935) were collected by Ohio State University in the 1930s on many plates, some used in more than one pipe. In some cases the plate

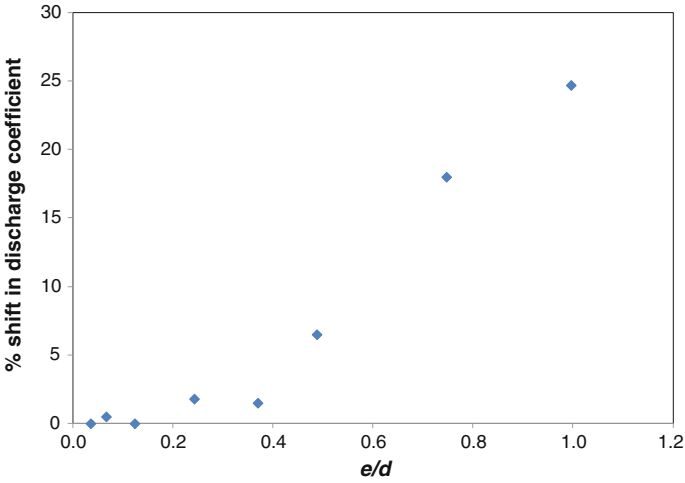


Fig. 2.7 Shift in discharge coefficient as a function of  $e/d$ : 4"  $\beta = 0.25$

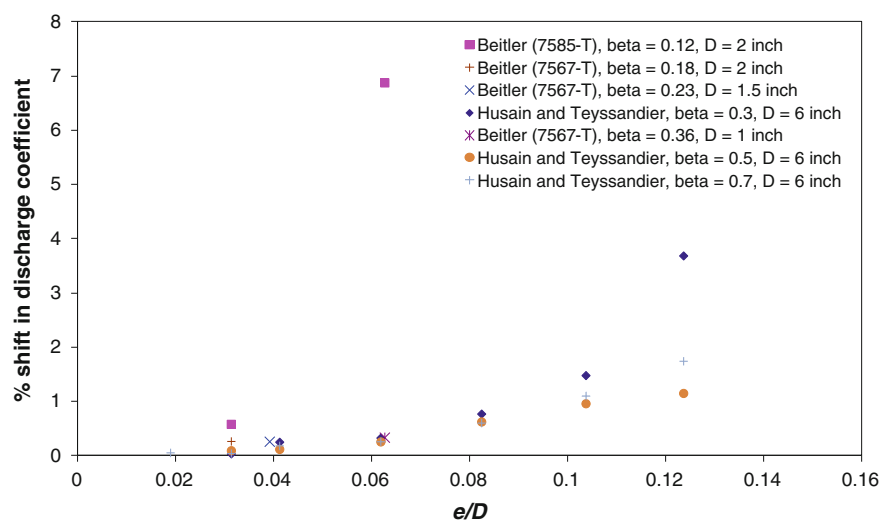
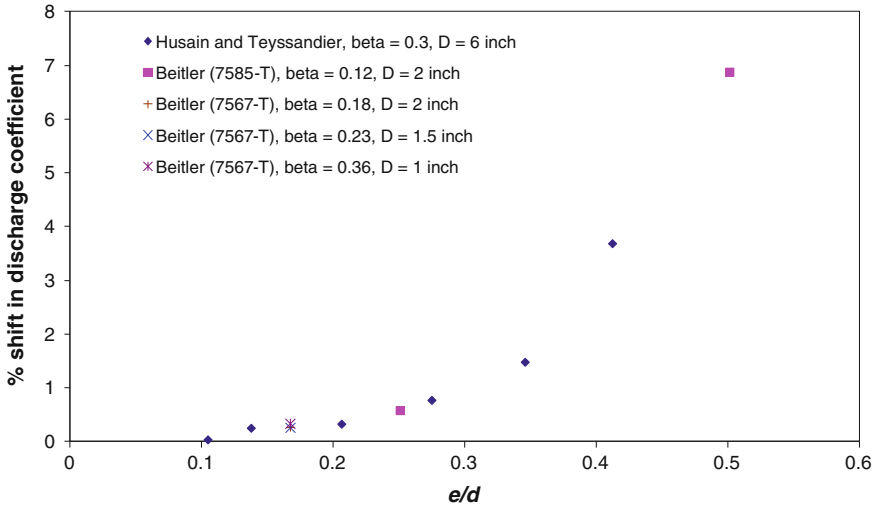


Fig. 2.8 Effect of changing  $e/D$

was re-bevelled to change the value of  $e$ . Those for small pipe diameters are presented in Reader-Harris et al. (2008). It is then possible using the points with  $e/d < 0.09$  as the baseline to plot the effect of  $e/D$  (see Fig. 2.8). A point from Beitler (7585-T,  $\beta = 0.12$ ,  $D = 2"$ ,  $e/d = 0.125$ ) was omitted because the spread of the deviations from the Reader-Harris/Gallagher (RG) (API) Equation (Eq. 5.23) for different Reynolds numbers was 1.39 %, more than three times the spread of the



**Fig. 2.9** Effect of orifice (bore) thickness ( $e$ ) for  $\beta < 0.4$ : shift in discharge coefficient from that obtained when  $e/d < 0.09$

deviations for any plotted points (except for the point from Beitler (7585-T),  $\beta = 0.12$ ,  $D = 2''$ ,  $e/D = 0.0625$ ). Where no points are available with  $e/d < 0.09$  the data are not plotted. For  $\beta \geq 0.2$  the ISO limit of  $e/D \leq 0.02$  is adequate, but for smaller  $\beta$  it is inadequate. The data for  $\beta$  up to 0.4 are plotted in Fig. 2.9 against  $e/d$ : a common curve for all data as a function of  $e/d$  is obtained. A new analysis of the OSU data for larger  $\beta$  and for larger  $D$  could be undertaken: the conclusions of Beitler (1935) are that there are two requirements: that  $e/d \leq 0.125$  and that  $el/h' \leq 0.25$ , where  $h'$  is the dam height, the distance from the sharp edge of the orifice plate to the nearest point of the pipe wall (i.e.  $h' = D(1 - \beta)/2$ ). The conclusions as regards requirements in Sect. 2.2.5.4 are more demanding than Beitler's and on the basis of the work here should prove adequate.

Husain and Goodson (1986) took data in 2" pipes with plates that are on the maximum limit in ISO 5167 for plate thickness or exceed it; these data show that an unbevelled plate with  $E = 3.57$  mm (5/32") did not significantly change its discharge coefficient when it was machined to be an unbevelled plate with  $E = 3.18$  mm (1/8") and then when it was bevelled with  $e = 0.79$  mm. Larger shifts would have been expected from Figs. 2.8 and 2.9.

#### 2.2.5.4 Requirements

On the basis of the work in Sects. 2.2.5.2 and 2.2.5.3 the requirements in ISO 5167-2:2003 are reasonable:

$$0.005D \leq e \leq 0.02D.$$

$$e \leq E \leq 0.05D.$$

However, there is an additional requirement that should be included in the next revision:

$$e \leq 0.1d.$$

This last requirement is only additional to the previous requirements when  $\beta < 0.2$ .

The angle of bevel makes no difference to the discharge coefficient, provided that it is  $45^\circ \pm 15^\circ$ . Husain and Goodson (1986) showed that having a  $30^\circ$  angle to the bore gave the same discharge coefficient as having a  $45^\circ$  angle; they also state that Ohio State data show that having a  $60^\circ$  angle to the bore makes a negligible difference from having a  $45^\circ$  angle [only data with a  $45^\circ$  bevel are given in Beitler (1935)].

If the plate is unbevelled ( $e = E$ ), then provided that both faces meet the specification for the front face and that flange or corner tappings are used the plate can be used bi-directionally. It will be fairly thin ( $E/D \leq 0.02$ ); so there may be issues with plate bending.

### 2.2.6 Circularity

The circularity of the orifice plate (and that of the pipe) is considered in Sect. 2.4.

## 2.3 The Pipe

### 2.3.1 General

The orifice plate can only be used as a flowmeter in accordance with ISO 5167 when it has upstream and downstream pipe (for an example see Fig. 2.10).

In addition to the effect of upstream (and downstream) fittings, considered in Chap. 8, it is necessary to consider

- the location of the pressure tappings (Sect. 2.3.2),
- the pipe roughness (Sect. 2.3.3),
- the effect of upstream steps (Sect. 2.3.4),
- the concentricity of the orifice plate in the pipe (Sect. 2.3.5)
- and the circularity and cylindricity of the pipe (see Sect. 2.4).

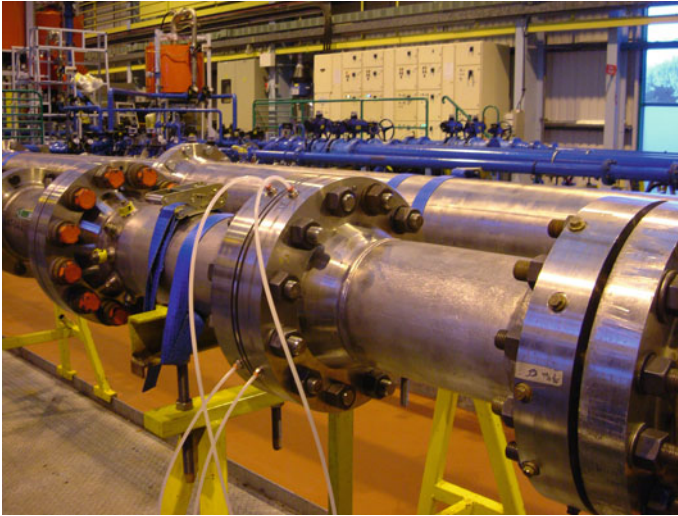


**Fig. 2.10** Orifice plate held between flanges

## 2.3.2 *Pressure Tappings*

### 2.3.2.1 General

In ISO 5167 there are three choices for the tappings: flange tappings (Sect. 2.3.2.2),  $D$  and  $D/2$  tappings (Sect. 2.3.2.2) and corner tappings (Sect. 2.3.2.3): see Fig. 2.11.

### 2.3.2.2 Flange and $D$ and $D/2$ Tappings

#### General

For fiscal oil and gas measurement flange tappings are normally specified: they are located in the flanges 25.4 mm (1") upstream of the upstream face of the plate and 25.4 mm (1") downstream of the downstream face of the plate. This distance will normally place them within the thickness of a flange holding the plate (see Fig. 2.12 for an example).

Flange tappings are generally the simplest in terms of manufacturing. Because of the large difference between the inside and outside diameters of the flanges no significant pressure expansion of the pipe will occur at the tappings and no correction in pipe diameter due to static pressure is required; moreover, the smaller the flow velocity is at the tapping, the less important are the roundness, sharpness and depth of the tappings (the main issues with tapping quality occur with Venturi tubes or throat-tapped nozzles: see Chaps. 7 and 9). The disadvantage in the use of orifice

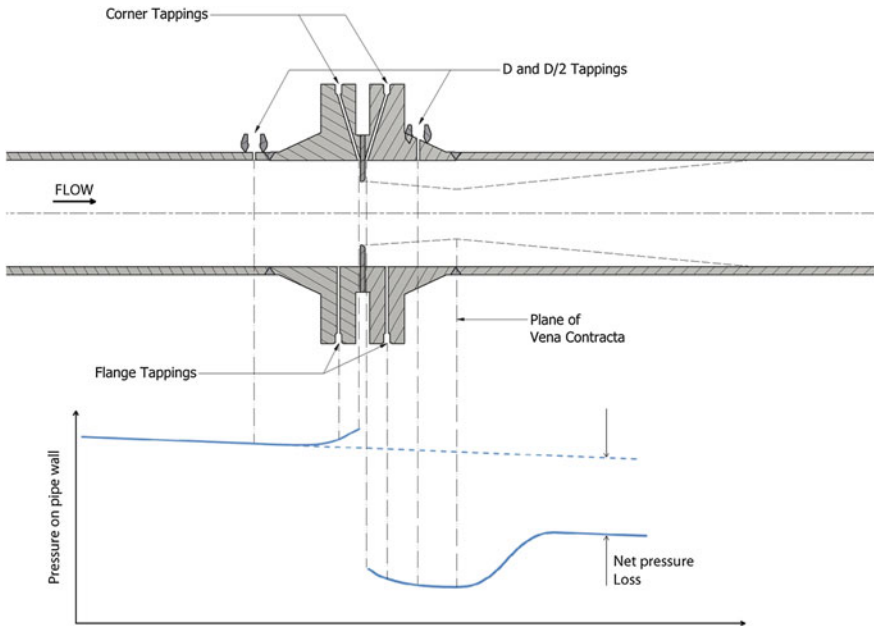
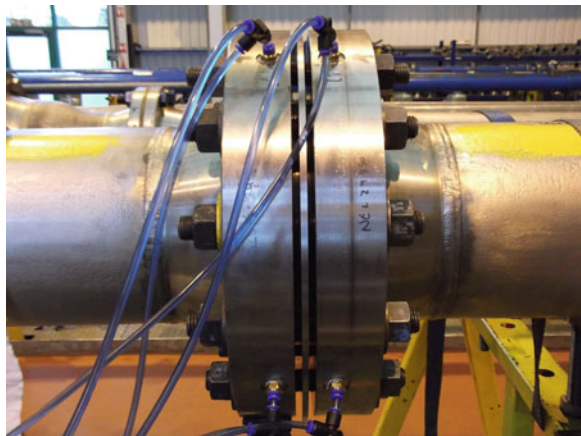


**Fig. 2.11** Flow through an orifice plate, showing the pressure tapping positions and approximate pressure profile

**Fig. 2.12** 8" orifice meter with flange tappings



plates with flange tappings is that because they are not geometrically similar they introduce additional complexity to the discharge-coefficient equation; moreover, they may be unsuitable for pipes smaller than those covered by ISO 5167-2:2003 (i.e.  $D < 50$  mm) because the downstream tapping might be in the pressure-recovery zone, which starts a little to the right of the *vena contracta* in Fig. 2.11.

For  $D$  and  $D/2$  tapplings the tapplings are located  $1D$  upstream and  $D/2$  downstream, both measured from the upstream face of the orifice plate: the upstream tapping is upstream of any disturbance to the pressure from the plate; the downstream tapping is near the pressure minimum for large  $\beta$ . Great care should be taken if tapplings are formed by welding a boss to a pipe wall that the welding heat does not create an internal bulge which alters the local velocity at the tapping as well as altering the pipe diameter at the tapping. Welding of bosses should be carried out prior to machining a bore, or an alternative method of preventing distortion employed.

### Tapping Diameter

For both flange and  $D$  and  $D/2$  tapplings the tapping diameter is not very critical as long as the centre of the tapping is correctly located: in 5.2.2.7 of ISO 5167-2:2003 the diameter must be less than both  $0.13D$  and 13 mm. In the equivalent API standard, API MPMS 14.3.2 (API 2000), the tapping diameters must be 9.5 mm (3/8") for 2" and 3" pipes and 12.7 mm (1/2") for 4" pipes and larger. When the data on which the discharge-coefficient equation is based were collected, all the European data were collected in tubes to ISO specification; the American data were collected in tubes to API specification: for example, for 2" tubes the European tapplings were generally 2 mm in diameter, i.e.  $0.04D$ , and the American tapplings were 9.5 mm (3/8") in diameter, i.e.  $0.19D$ . There was no noticeable difference between European data and American data: the mean deviation for European water data from the Reader-Harris/Gallagher (1998) Equation was 0.005 %, for American water data it was 0.008 %. All the 3" data were American (with tapplings 9.5 mm (3/8") in diameter, i.e.  $0.122D$ ) and 95 % of the 3" data are within about 0.26 % of the Reader-Harris/Gallagher (1998) Equation in ISO 5167-2:2003, an exceptionally good result. So there was no sign that tapping diameter had much effect on the discharge coefficient.

### Tapping Location

The tolerances on location are given in 5.2.2.2 and 5.2.2.3 of ISO 5167-2:2003. The permitted upstream and downstream spacings for flange tapplings are:

25.4 mm  $\pm$  0.5 mm when  $\beta > 0.6$  and  $D < 150$  mm

25.4 mm  $\pm$  1 mm in all other cases, i.e.  $\beta \leq 0.6$ , or  $\beta > 0.6$ , but  $150 \text{ mm} \leq D \leq 1000 \text{ mm}$

The Reader-Harris/Gallagher (1998) Equation (Eq. 5.22a, 5.22b) can be used to calculate the effect of moving the tapplings: the effect is shown in Figs. 2.13 and 2.14. In Eq. 5.22a, 5.22b  $A$  was taken as 0; this gives the maximum shift.

Work has also been carried out by Zedan and Teyssandier (1990).

From Figs. 2.13 and 2.14 the largest errors can occur for large  $\beta$  at the upstream flange-tapping location.



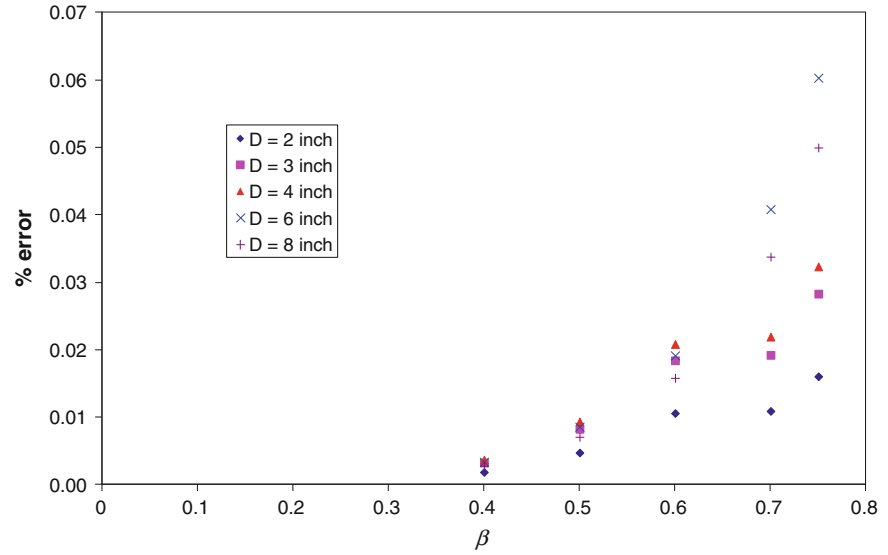


**Fig. 2.13** Maximum absolute error due to permissible variation of ISO upstream flange-tapping location

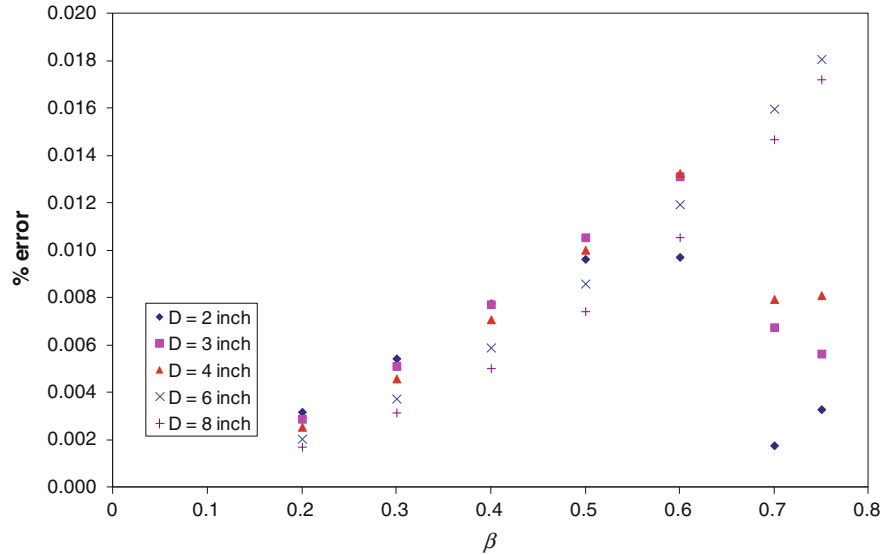


**Fig. 2.14** Maximum absolute error due to permissible variation of ISO downstream flange-tapping location

Because the pressure profile is very flat both  $D$  upstream of the orifice plate and near the vena contracta the effect of small errors in the location of  $D$  and  $D/2$  tapings is very small.

### 2.3.2.3 Corner Tappings

Corner tapings are located in the corners between the plate and the pipe wall. They may be either single tapings or annular slots. In 5.2.3.3 of ISO 5167-2:2003 the three lines headed ‘For clean fluids and vapours’ give requirements for sizes of corner tapings based on geometrical similarity to the original orifice runs on which the discharge coefficient is based. As  $\beta$  increases the discharge coefficient changes more rapidly with tapping position (as can be seen from the Reader-Harris/Gallagher (1998) Equation) and so the orifice meters need to be closer to the original ones. However, it was accepted that to require a tapping size of a maximum of 1 mm was not sensible; so for  $D < 100$  mm values up to 2 mm are acceptable even if not permitted by instructions 1 or 2 in 5.2.3.3 of ISO 5167-2:2003. The three lines headed ‘For any values of  $\beta$ ’ give requirements based on what is sensible for particular fluids. For certain fluids in certain sizes it is not possible to design a system using single corner tapings that is compliant with ISO 5167.

Except for pipes smaller than those covered by ISO 5167-2:2003 flange tapings are much more commonly used than corner tapings.

NOTE Corner tapings may be installed in a carrier ring: this is shown in Fig. 4 of ISO 5167-2:2003. The permitted diameter of the carrier ring is given in 5.2.3.6 of ISO 5167-2:2003. If the tapings are installed in a carrier ring then differences between the ring diameter and that of the pipe become important: see 7.3 of ISO/TR 12767:2007.

### 2.3.2.4 Number of Tapings

Single tapings or multiple tapings in each tapping plane are permitted. If there are 4 tapings in each tapping plane, those in each tapping plane should be connected in a triple-T arrangement as in Fig. 4.8. If there is an asymmetric flow profile the triple-Ts reduce the effect of upstream installation. However, if there is any risk of liquid in a gas flow tapings should only be in the top half of the pipe, and in practice a single tapping on the side or on the top is common. If there is any risk of gas in a liquid flow tapings should only be in the bottom half of the pipe. See Sect. 4.2.2 for more details.

See ISO 2186:2007 (ISO 2007a) for more information on steam measurement with orifice plates.

### 2.3.3 Pipe Roughness

#### 2.3.3.1 Uniform Roughness

New roughness limits for pipework upstream of orifice plates were included in ISO 5167-2:2003. These are derived from a physical understanding of the effect of pipe roughness on orifice plate discharge coefficients and the knowledge of the roughness of the pipes on which the discharge-coefficient equation in ISO 5167-2:2003 is based. The physical understanding was obtained from computational work at NEL (Reader-Harris and Keegans 1986; Reader-Harris 1990). Pipe roughness limits have been calculated to ensure that roughness will not shift the discharge coefficient from that given by the discharge-coefficient equation by more than an appropriate fraction of its uncertainty.

The friction factor,  $\lambda$ , can be measured directly (see Sect. 1.5), using:

$$\Delta p = \frac{\lambda \rho \bar{u}^2 x}{2D} \quad (1.19)$$

where  $\Delta p$  is the difference in pressure between two tappings spaced a distance  $x$  apart in a pipe of diameter  $D$  and  $\bar{u}$  is the mean velocity in the pipe. It is simpler to measure the arithmetic mean deviation of the roughness profile,  $R_a$ , (the average of the absolute values of the deviation from the mean), to deduce the uniform equivalent roughness,  $k$ , by taking it to be approximately equal to  $\pi R_a$  (based on the assumption that the wall has a sinusoidal profile) and to calculate  $\lambda$  using the Colebrook-White Equation (Schlichting 1960):

$$\frac{1}{\sqrt{\lambda}} = 1.74 - 2 \lg \left( \frac{2k}{D} + \frac{18.7}{Re_D \sqrt{\lambda}} \right) \quad (1.21)$$

(following ISO 80000-2:2009,  $\log_{10}$  is written  $\lg$ ).

The arithmetic mean deviation of the roughness profile,  $R_a$ , or the friction factor,  $\lambda$ , (or both) was measured for each of the pipes used to collect the data to which the discharge-coefficient equation was fitted. Values of roughness are given in the reports listed in Chap. 5. The API (US) pipes had rms ( $R_q$ ) approximately 1–6  $\mu\text{m}$  ( $R_a$  values would be similar, probably slightly smaller) (Whetstone et al. 1989).

NOTE When the 24" pipework ( $D = 585.95$  mm) for the orifice equation tests was made British Gas (Stewart 1989) measured both its  $R_a$  value, obtaining 4.2, 6.1, 5.5 and 3.3  $\mu\text{m}$  at four locations along it, an average of 4.8  $\mu\text{m}$ , and the pressure loss along it, which gave a friction factor of 0.0095 at a Reynolds number of  $2.8 \times 10^7$ , which corresponded to  $k = 13.8$   $\mu\text{m}$ . On this occasion  $k/R_a = 2.9$ , in good agreement with expectation.

Using the measurements of pipe roughness it was possible to fit a discharge-coefficient equation containing an explicit friction factor term; this was done at the time when the PR14 Equation (see Chap. 5) was developed and, using the PR14

tapping terms, the following equation for the  $C_\infty$  and slope terms was obtained for  $Re_D > 3700$  (see Eq. 5.C.4):

$$C_\infty + C_s = 0.5945 + 0.0157\beta^{1.3} - 0.2417\beta^8 + 0.000514(10^6\beta/Re_D)^{0.7} \\ + (3.134 + 4.726A')\beta^{3.5}\lambda \\ \text{where} \quad (2.2) \\ A' = \left( \frac{2100\beta}{Re_D} \right)^{0.9}.$$

This gives the change in discharge coefficient due to roughness,  $\Delta C_{\text{rough}}$ , as

$$\Delta C_{\text{rough}} = 3.134\beta^{3.5}\Delta\lambda \quad (2.3)$$

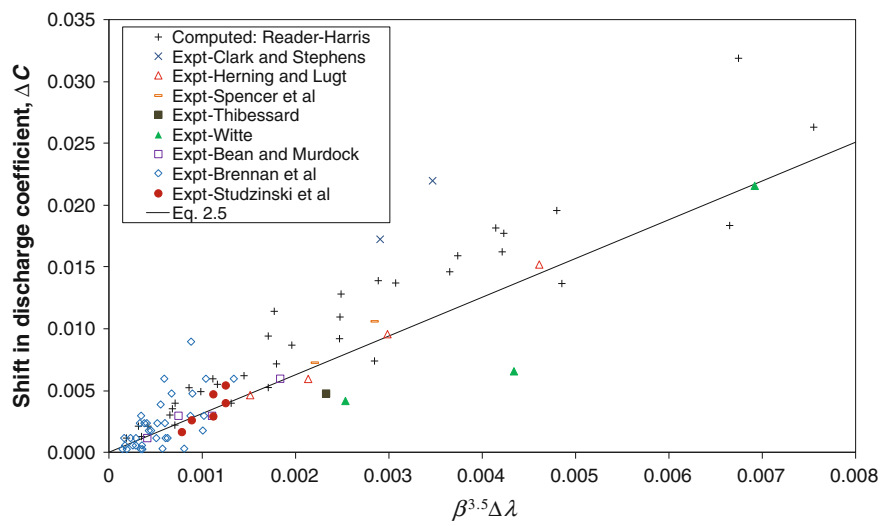
provided that  $Re_d$  is sufficiently large that  $A'$  is negligible. This equation was evaluated by Morrow and Morrison (1999): ‘they compared the CFD results with the Reader-Harris correlation. The changes in pipe roughness and  $C_d$  values were in agreement with the equation predictions of Reader-Harris. They also found that the new Reader-Harris equation compensates for systematic variations of  $C_d$  with the  $\beta$  ratio that have been included in the past equations’ (Morrow et al. 2002).

Figure 2.15 gives measured and computed (using CFD) values of  $\Delta C$  as a function of  $\beta^{3.5}\Delta\lambda$ . The computed values (Reader-Harris 1990) and the European experimental data (Clark and Stephens 1957; Herning and Lugt 1958; Spencer et al. 1969; Thibessard 1960; Witte 1953) were obtained using corner tapings. The North American experimental data (Bean and Murdock 1959; Brennan et al. 1989; Studzinski et al. 1990) were obtained using flange tapings. In computational work the effect of roughness on discharge coefficients obtained with different pairs of pressure tapings was considered and it was shown that the effect of pipe roughness on the discharge coefficient using  $D$  and  $D/2$  tapings is about 25 % less than on that using corner tapings. Since all the computational and most of the experimental data in Fig. 2.15 were collected using corner tapings this may explain why Eq. 2.3 lies below the majority of the plotted data.

Nevertheless there is a large scatter in the plotted data, and so a single equation is used to describe the effect of pipe roughness for all tapings. The equation used to determine limits of pipe roughness is again taken from Eq. 2.2, but the  $A'$  term is included:

$$\Delta C_{\text{rough}} = (3.134 + 4.726A')\beta^{3.5}\Delta\lambda \quad (2.4)$$

It is not known whether the effect of change in friction factor increases for small Reynolds number, but it is safer to include the term in  $A'$  in calculating the limits of pipe roughness. Moreover, there is little disadvantage in its inclusion since it causes a slight reduction in the limits of pipe roughness in a range of Reynolds number where they are already wide.



**Fig. 2.15** The effect of rough pipe on the orifice plate discharge coefficient

In order to calculate the limits of pipe roughness for the discharge-coefficient equation in ISO 5167-2:2003, it is necessary to use the measured values of relative roughness for each pipe used to collect the data to obtain an approximate mean pipe relative roughness for the data (and thus for the equation fitted to it). The mean pipe relative roughness is a function of  $Re_D$ : the estimates are given in Table 2.1.  $k/D$  reduces with  $Re_D$  because the higher Reynolds numbers generally occurred in the larger pipes, which were generally relatively smoother. The values of friction factor are consistent with the values of relative roughness if the Colebrook-White Equation is used.

The maximum permissible shift in  $C$  depends on  $U$ , the stated uncertainty of  $C$ . It is assumed here that the percentage shift,  $P$ , should not exceed the values in Table 2.2.

**Table 2.1** Values of  $k/D$  and  $\lambda$  associated with the Reader-Harris/Gallagher (1998) Equation

$Re_D$	$10^4$	$3 \times 10^4$	$10^5$	$3 \times 10^5$	$10^6$	$3 \times 10^6$	$10^7$	$3 \times 10^7$	$10^8$
$10^4 k/D$	1.75	1.45	1.15	0.9	0.7	0.55	0.45	0.35	0.25
$\lambda$	0.031	0.024	0.0185	0.0155	0.013	0.0115	0.0105	0.010	0.0095

**Table 2.2** Maximum permissible percentage shift,  $P$ , in  $C$  due to pipe roughness

$P$	$\beta$
$0.5\beta$	$\beta \leq 0.5$
0.25	$0.5 < \beta \leq 0.6$
$0.5(1.667\beta - 0.5)$	$0.6 < \beta \leq 0.71$
$1.13\beta^{3.5}$	$0.71 < \beta$

This restriction ensures that for  $\beta \leq 0.5$ , where other sources of error are dominant,  $P/U < \beta$ ; for  $0.5 < \beta \leq 0.71$   $P/U < 0.5$ ; for  $0.71 < \beta$  the maximum value of  $P/U$  increases from 0.5 at  $\beta = 0.71$  to 0.55 at  $\beta = 0.75$ .

Given the value of  $P$  in Table 2.2 and the value of  $\lambda$  associated with the data in the database (and thus with the equation) in Table 2.1, it is possible from Eq. 2.4 to calculate the maximum and minimum values of  $\lambda$  and hence of  $k/D$  for use with the equation for each  $Re_D$  and  $\beta$ . It was decided to write ISO 5167:2003 in terms of  $R_a$  rather than  $k$  for specification of pipe roughness, since this is more convenient for users, although  $k$  is still mentioned. The maximum and minimum values of  $R_a/D$  for pipes upstream of orifice plates are given in Tables 1 and 2 of ISO 5167-2:2003.

It is stated in ISO 5167-2:2003 that the roughness requirements are satisfied in both the following cases:

$$1 \mu\text{m} \leq R_a \leq 6 \mu\text{m}, D \geq 150 \text{ mm}, \beta \leq 0.6 \text{ and } Re_D \leq 5 \times 10^7.$$

$$1.5 \mu\text{m} \leq R_a \leq 6 \mu\text{m}, D \geq 150 \text{ mm}, \beta \leq 0.6 \text{ and } Re_D \leq 1.5 \times 10^7.$$

These are not additional restrictions, just a method of removing the need to use Tables 1 and 2 of ISO 5167-2:2003 in some cases.

The tables prescribe  $k/D \leq 0.005$  even if the calculated value is higher. Although the limits for very large  $Re_D$  are much tighter than those in ISO 5167-1:1991, for  $Re_D = 3 \times 10^5$  they are very similar; this is unsurprising since the limits in ISO 5167-1:1991 were probably derived from data collected at around that Reynolds number. The fact that the original orifice meters were not hydraulically smooth means that in some situations a hydraulically smooth pipe is too smooth for the Reader-Harris/Gallagher (1998) Equation to be used without additional uncertainty. The minimum values for relative pipe roughness in Table 2 of ISO 5167-2:2003 represent exceedingly smooth pipes.

It might be argued that an equation with a friction factor term included explicitly should have a lower uncertainty. Such an equation was rejected on the grounds that it would be difficult to use.

### 2.3.3.2 Rough Pipes with a Smooth Portion Immediately Upstream of the Orifice

The tests of Clark and Stephens (1957) included the effect of extremely rough pipes (e.g. ones with peas stuck to them) and also the effect of cleaning:  $5D$  of clean pipe upstream of the orifice plate reduced the error due to roughness to about a tenth of what it would have been. Where significant change in roughness over time might be expected a possible strategy might be to use stainless steel pipe for the pipe immediately upstream of the plate, carbon steel further upstream.

To examine the effect of a smooth section of pipe immediately upstream of an orifice plate tests were undertaken at SwRI (Morrow et al. 2002) in a 4" pipe.

Baseline data were taken with the whole upstream pipe of roughness  $R_a = 1.27 \mu\text{m}$  (50  $\mu\text{in.}$ ). The pipe from  $10D$  to  $45D$  upstream of the orifice plate was then roughened: the pipe roughness increased from 1.27 to  $18.3 \mu\text{m}$  (50 to 719  $\mu\text{in.}$ ). With  $\beta = 0.67$  the results were very similar to the baseline (a shift in discharge coefficient of 0.15 % in magnitude at most). This suggests that cleaning the last  $10D$  of a pipe will in many cases be sufficient.

When two high-performance flow conditioners were included in turn  $10D$  upstream of the orifice plate in the baseline pipe the data were very close to the baseline; when the same flow conditioners were included in turn  $10D$  upstream of the orifice plate with roughened pipe from  $10D$  to  $45D$  upstream of the orifice plate the data were again very close to the baseline. This suggests that rough pipe upstream of a flow conditioner does not spoil its performance.

The final set of tests were carried out with the pipe rough [ $R_a = 18.3 \mu\text{m}$  (719  $\mu\text{in.}$ )] all the way from  $45D$  upstream to the orifice plate: with  $\beta = 0.67$  the shift in discharge coefficient was an increase of about 1.7 %. Inserting the two high-performance flow conditioners in turn  $10D$  upstream of the orifice plate with rough pipe upstream and downstream of the flow conditioner gave a shift from the smooth baseline at least as large as had been obtained with a rough pipe and no flow conditioner and in some cases almost twice as large. So whereas rough pipe upstream of the flow conditioner has very little effect, rough pipe downstream of the flow conditioner may have a very significant effect.

### 2.3.3.3 Non-uniform Roughness

In practice roughness is often non-uniform, because in gas pipelines liquid is particularly present on the bottom of the pipe. Before undertaking research in this area video recordings of the inside of 10" pipes (230 mm ID) were kindly lent to NEL by BP Amoco, and from these it was concluded that it would not be unreasonable to assume that values of roughness height  $k$  of the order of 0.5 mm would be possible. Accordingly experiments were undertaken with the same level of relative roughness as had been found in these pipes (Reader-Harris et al. 2003).

To achieve the same relative roughness in a 4" pipe as had been found by BP Amoco gave  $k$  of the order of 0.2 mm. This corresponds to a P80 Sandpaper (actually silicon carbide paper, commonly called wet and dry paper) with a grain size of 197  $\mu\text{m}$ . It was decided to work also with a smoother sandpaper (P240) with a grain size of 60  $\mu\text{m}$ . Sandpaper of each roughness was obtained and glued to the inside of the pipe from  $\frac{1}{2}D$  upstream of the orifice plate to  $10D$  upstream of it. As shown in Sect. 2.3.3.2 the discharge coefficient is largely affected by the pipe roughness over the  $10D$  upstream of the orifice plate, and it was necessary to leave 25 mm clean upstream of the flange tapplings as the sandpaper was simply glued to the surface. Flange Tapplings D were at the bottom of the pipe (see Fig. 2.16) and except where the whole pipe was rough the sandpaper was at the bottom of the pipe and symmetrical about the bottom of the pipe. It was not simple to ensure that the sandpaper remained stuck to the surface, but with the rougher sandpaper data were

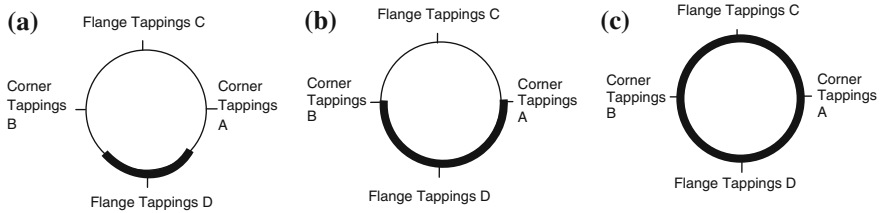


**Fig. 2.16** Roughened portions of pipes relative to the pressure tapplings. **a** Quarter pipe roughened. **b** Half pipe roughened. **c** Whole pipe roughened

obtained in which the sandpaper remained satisfactorily stuck to the walls. The smoother sandpaper was generally weaker, and so in addition to its tendency to become unstuck it also became wavy in use, and no satisfactory data could be obtained.

The data obtained with the rougher sandpaper are presented in Fig. 2.17. It is interesting that similar data are obtained with each pair of tapplings and that the shift is approximately proportional to the fraction of the pipe which is rough. According to Eq. 2.3 for uniformly rough pipe the predicted shift in discharge coefficient at  $Re_D = 2.74 \times 10^5$  was 1.26 %, using the Colebrook-White Equation (Eq. 1.21) to determine the friction factor and assuming that the smooth pipe had  $R_a = 0.8 \mu\text{m}$  and that  $k = \pi R_a$ . Additionally it would be expected that for entirely rough pipe the thickness of the roughness elements and the paper might increase the shift in discharge coefficient by 0.4 %. So the measured shift in discharge coefficient of 1.98 % compares quite well with the predicted value of 1.66 %.

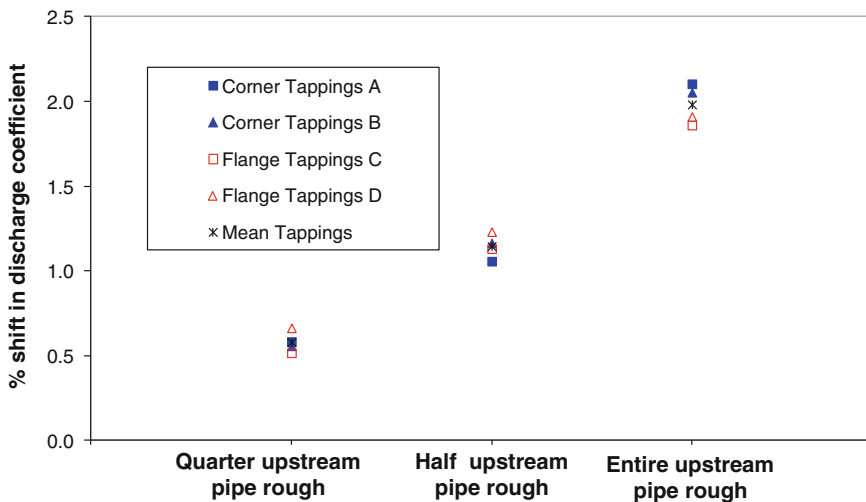


**Fig. 2.17** % shift in discharge coefficient due to rough pipe upstream of an orifice plate ( $\beta = 0.67$ )



### 2.3.4 Steps and Misalignment

Over the first  $2D$  of the pipe upstream of the orifice no measured diameter of the pipe is permitted to differ by more than 0.3 % from  $D$ , the mean diameter of the pipe (see 6.4.2 of ISO 5167-2:2003 and Sect. 2.4). To be consistent with ISO 5167-2:2003 a protruding weld should not cause a change in measured diameter greater than 0.3 %; if it is greater than this value the weld bead should be removed.

The basis on which this requirement was derived is not clear, but Teyssandier (1985) considered the effect of steps or gaps  $D/4$  wide adjacent to an orifice plate or  $2D$  upstream of it in a 2" pipe. As far as these data are concerned a limit of 0.3 % in maximum permissible step as in ISO 5167-2:2003 appears conservative.

Beyond  $2D$  from the orifice the standard is less clear. The rules on steps are clear, if rather complicated. They result from NEL tests (Reader-Harris and Brunton 2002): Fig. 2.18 shows the shift in discharge coefficient where pipes of different schedule were placed at different distances upstream of a schedule 40 pipe: the effect of a contraction by about 5 % of  $D$  (Schedule 10 to Schedule 40) is much less than the effect of an expansion by about 5 % of  $D$  (Schedule 80 to Schedule 40). The data point for a Schedule 40 pipe shown in the figure was taken using an ordinary Schedule 40 pipe, whereas the baseline pipe was honed. 6.4.3 of ISO 5167-2:2003 permits steps of up to 0.3 % of  $D$  beyond  $2D$  from the orifice plate and up to 2 % of  $D$  beyond  $10D$  from the orifice plate. If the step is a contraction it permits steps of up to 6 % of  $D$  beyond  $10D$  from the orifice plate. It also permits steps (expansions or, of course, contractions) of up to 6 % of  $D$  beyond the closest permissible location for the insertion of an expander provided that the step is also at

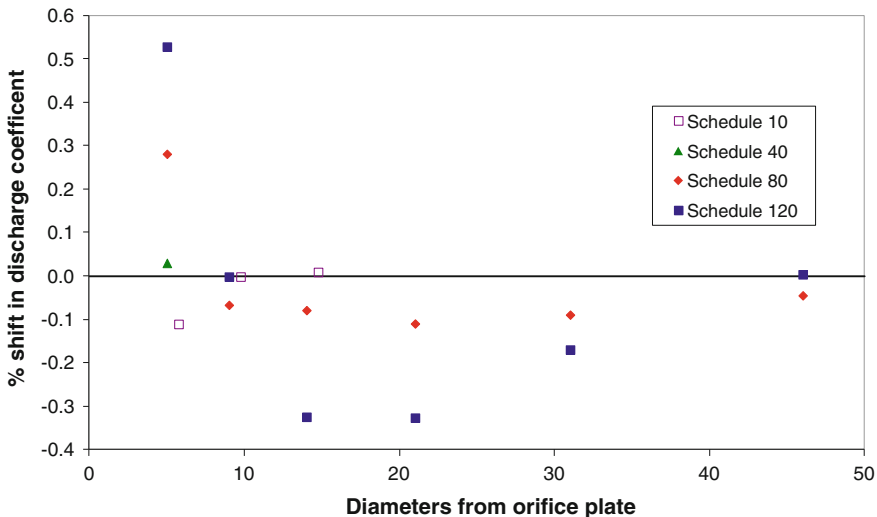


**Fig. 2.18** Upstream steps: % shift in discharge coefficient due to pipes at various distances upstream of an orifice plate ( $\beta = 0.67$ ) in a Schedule 40 pipe (Reader-Harris and Brunton 2002)

least  $10D$  from the orifice plate. Although larger steps could be used satisfactorily for sufficiently small  $\beta$  it is generally wise to design a system so that  $\beta$  may be easily changed if the flow is higher or lower than the design flow.

The aim of these changes to ISO 5167 was to avoid the requirement to use machined pipes beyond  $10D$  from the orifice. Moreover, a change of 6 % of  $D$  generally permits a change from one common pipe schedule to the next. The NEL tests provide justification for common practice in calibration laboratories where upstream pipes of the same nominal diameter but larger internal diameter than the customer's meter are used  $25D$ , say, upstream of the meter.

The steps in Reader-Harris and Brunton (2002) were concentric steps, but at steps there may be offsets as well: 6.4.3 of ISO 5167-2:2003 states that the actual step caused by misalignment and/or change in diameter shall not exceed the permitted diameter step at any point of the circumference. To meet these restrictions will probably require the use of dowels or the equivalent to ensure alignment. If it is intended to machine the pipe immediately upstream of the orifice plate but not to machine the pipe upstream of that then the latter pipe should be selected to be sufficiently cylindrical that the former pipe can be machined to a diameter such that where the flanges meet there is a sufficiently small step. If the pipe immediately upstream of the orifice plate is manufactured first then the pipe upstream of that may require machining, and it may be necessary to buy a thicker walled pipe to machine.

What is not clear are the rules where the internal diameter of the upstream pipe changes not suddenly (as with a step) but gradually. This is not permitted in the first  $2D$  upstream of the orifice plate. If the diameter change occurs more than  $2D$  away it is not clear what is permitted. The standard is not clear because of a lack of experimental data. What often results in poor practice is to buy a pipe for installation immediately upstream of the orifice, measure it, find it insufficiently cylindrical, machine the first  $2D$  until it is sufficiently cylindrical, and then blend the machined and unmachined diameters at  $2D$ . The problem with this is that it leaves an expansion  $2D$  upstream of the orifice. It is much better to work the other way round, i.e. to start with an upstream pipe a little shorter than is required, to weld a piece of thicker-walled pipe to the upstream pipe (the thicker-walled pipe is to be adjacent to the orifice plate) and to machine the thicker-walled pipe so that it approximately matches the rest of the upstream pipe and there is very small deviation from constant diameter and concentricity where the machined and unmachined sections are blended. For 2" orifice meters it is reasonable to machine the whole upstream length; for 24" meters it is desirable either to select the pipework so that no machining is required or to have it manufactured to the required tolerance; for 8" meters machining of a part of the upstream length is probably required.

Goodson et al. (2004) studied the effect of recesses corresponding to those formed where an RTJ-flanged orifice fitting is joined to an upstream meter tube: tests in 4" ( $\beta = 0.2, 0.4$  and  $0.67$ ) and 8" ( $\beta = 0.67$ ) showed that the effect of the recesses was negligible.

If gaskets (rather than 'O' rings) are used between pipes or at the orifice it is important that they do not protrude into the pipe; therefore, in practice there will be a small recess. 5.2.6.6 of ISO/TR 9464:2008 recommends that at the plate a gasket

be not thicker than  $0.03D$ ; such a gasket will have a negligible effect on the discharge coefficient.

Straightness of the upstream pipe is defined by 7.1.3 of ISO 5167-1:2003, and is normally checked visually.

The downstream pipe diameter is much less critical: 6.4.6 of ISO 5167-2:2003 states that it only needs to be within 3 % of that of the upstream pipe: Teyssandier (1985), using a 2" orifice meter with flange tapplings, looked at the effect of a protrusion or a recess  $D/4$  wide at the orifice plate on its downstream side and found that for  $\beta = 0.3$  or  $0.5$  its effect is less in magnitude than 0.1 % for protrusions or recesses up to  $0.0625D$  in height (or depth) and less in magnitude than 0.2 % for protrusions or recesses up to  $0.125D$  in height (or depth); for  $\beta = 0.7$  its effect is less in magnitude than 0.1 % for a protrusion up to  $0.03125D$  in height or a recess up to  $0.0625D$  in depth. From those data it can be seen that provided that a protrusion is less than 20 % of the dam height its effect is less than 0.1 %; it is not surprising that the effect increases rapidly when the protrusion is a large percentage of the dam height (at 83 % of the dam height for  $\beta = 0.7$  the effect is 5.25 %); at 100 % of the dam height a thick plate is obtained. The dam height is the distance from the sharp edge of the orifice plate to the nearest point of the pipe wall, i.e.  $\frac{D(1-\beta)}{2}$ . Teyssandier (1985) also looked at the effect of a protrusion or a recess  $D/4$  wide  $2D$  downstream of the orifice plate and found that even a protrusion  $0.125D$  in height for  $\beta = 0.7$  had an effect of only 0.1 %.

In conclusion, the rules on steps are given in 6.4 of ISO 5167-2:2003. They are rather complicated; an explanation for much of their complexity has been given in this section.

### 2.3.5 Eccentricity

The orifice plate and the pipe need to be close to concentric. The effect of eccentricity has been measured by Norman et al. (1984), Husain and Teyssandier (1986a) and Miller and Kneisel (1968). The eccentricity (i.e. the distance between the centre-line of the pipe and that of the orifice) is generally non-dimensionalized with  $D/(0.1 + 2.3\beta^4)$ . This non-dimensionalization was used in ISO 5167:1980 (ISO 1980). When an orifice plate with a single tapping upstream and downstream is used the effect of eccentricity is greater in the direction parallel to the tapplings than in the direction perpendicular to them. The limit on eccentricity in ISO 5167-2:2003 parallel to the tapplings is

$$\frac{0.0025D}{0.1 + 2.3\beta^4} \quad (2.5)$$

and that in the direction perpendicular to the tapplings is twice that.

NOTE The limit in ISO 5167:1980 was  $0.0005D/(0.1 + 2.3\beta^4)$  in all directions. In ISO 5167-1:1991 (ISO 1991) it was increased to  $0.0025D/(0.1 + 2.3\beta^4)$  in all directions. In ISO 5167-2:2003 it remained unchanged parallel to the tapplings but was increased perpendicular to the tapplings.

In 2.6.2.1 of API MPMS 14.3.2 the same limit as in Eq. 2.5 is applied parallel to the pressure tapplings, but in the direction perpendicular to the pressure tapplings the limit is four times that in Eq. 2.5. The ISO limit according to Fig. 6 of ISO/TR 12767:2007 gives shifts in the perpendicular direction up to about 0.08 % in magnitude, the API up to about 0.15 %. API MPMS 14.3.2 allows twice as large a limit if tapplings 180° apart are connected; however, Fig. 6 of ISO/TR 12767:2007 shows that sometimes there is no cancellation. The ISO limits appear reasonable.

If the eccentricity is close to the limit, determining whether the eccentricity is inside or outside the limit is not trivial: if the plate is held between three dowels the deviation between the centreline of the orifice and that of the outside of the orifice plate, the deviation between the centreline of the pipe and the centre of the circle formed by the inside of the dowels, and the possible variation in the location of the plate within the dowels will all have to be considered.

On one occasion an orifice plate was installed so eccentrically that there was flow past the outside of the plate: this problem was investigated by Barton et al. (2005).

According to 6.5.2 of ISO 5167-2:2003 the plate shall be perpendicular to the pipe centreline within 1°. Whether this is based on engineering judgment or on experiment is not clear. This requirement should be stated when specifying alignment of flanges being welded during fabrication.

## 2.4 Dimensional Measurements

Where an orifice plate is being used without flow calibration the dimensional measurements are crucial to the calculated flowrate. The value for orifice diameter used in Eq. 1.15 is the mean of at least four measurements of diameter in different orientations (5.1.8.2 of ISO 5167-2:2003). 6.4.2 of ISO 5167-2:2003 requires that at least four measurements of diameter be made in each of three planes in the pipe. ISO 5167-2:2003 gives limits on the variation in diameters permitted, but measured uncertainties lower than the maximum permitted in ISO 5167-2:2003 can be used in the uncertainty of the mass flowrate (see Sect. 4.8). Modern coordinate measuring machines often do not give individual diameters but give a mean diameter and circularity; nevertheless, it can easily be checked whether the measurements meet the intention of ISO 5167-2:2003. For the pipe the mean diameter is obtained from the average of measurements made in at least three planes over a distance of  $0.5D$  upstream of the upstream pressure tapping: one plane must be at  $0D$ , one at  $0.5D$ , from the upstream tapping and one in the plane of the weld in the case of a weldneck construction.

The measurements of the orifice are considerably more important than those of the upstream pipe (see Eq. 4.13 in Sect. 4.8): no orifice diameter may differ by more than 0.05 % from the mean, whereas in the pipe the tolerance is 0.3 %. In practice this is a minimum requirement. One of the advantages of orifice metering is that the diameter in the discharge-coefficient equation is that of the orifice plate. Where  $\beta$  is small a low quality pipe is acceptable, provided that the orifice plate is of high quality. For larger  $\beta$  the effect of any error in pipe diameter becomes more significant: from Eq. 4.13 the effect can be approximately calculated.

## 2.5 Orifice Fittings

The orifice fitting, which enables the operator to change or remove an orifice plate easily (i.e. without undoing flange bolts), was introduced by Paul Daniel. Tests were undertaken in 1949–51 in Rockville by the joint AGA-ASME committee to compare measurement uncertainty using orifice fittings with that obtained using plates held between flanges (AGA 1951, 1954a). Tests were also carried out as part of the Refugio tests in 1952/3: an orifice plate held between flanges (an orifice flange union) and an orifice fitting were placed in a 30" line, the former upstream of the eight 10" reference meters and the latter downstream, and 'it was unanimously concluded that the equations for computing coefficients of discharge in AGA Gas Measurement Report No 2 may be used, within the tolerances given, for large diameter meter tubes (e.g., 30-in.) using either orifice flange unions or orifice fittings' (AGA 1954b).

A picture of an orifice plate emerging from an orifice fitting is shown as Fig. 2.19.

Some systems are designed so that an orifice plate may be changed without depressurizing the line.

**Fig. 2.19** Orifice plate emerging from an orifice fitting



## 2.6 Pressure Loss

The pressure loss is required for hydraulic system design, but a more accurate value is required if the pressure loss ratio (the ratio of the pressure loss to the differential pressure) is to be used for diagnostic purposes (see Sect. 4.10).

The pressure loss for an orifice plate is calculated as follows. The reader is warned that this section is more mathematically complex than the rest of the book.

The momentum theorem is obtained by integrating the equation of motion over a fixed volume so that

$$\rho \frac{Du_i}{Dt} = \rho F_i + \frac{\partial \sigma_{ij}}{\partial x_j}, \quad (2.6)$$

where  $\rho$  is the density,  $u_i$  the velocity in the  $x_i$ -direction,  $F_i$  the body force,  $\sigma_{ij}$  the stress tensor and  $D/Dt$  the derivative following the motion of the fluid, becomes, on expanding the derivative following the motion of the fluid and using mass conservation and the divergence theorem,

$$\iiint_V \frac{\partial(u_i \rho)}{\partial t} dV = - \iint_A \rho u_i u_j n_j dA + \iiint_V F_i \rho dV + \iint_A \sigma_{ij} n_j dA \quad (2.7)$$

where the fixed volume  $V$  is bounded by surface  $A$ .

The stress tensor consists of two terms: the pressure term is sufficient for the approximation here, so  $\sigma_{ij} = -p\delta_{ij}$ . The flow is steady and the body force (gravity) makes a contribution to the pressure which will make no contribution to the pressure loss.

Equation 2.7 is applied to the volume marked  $V$  on Fig. 2.20. Equations are supplied for incompressible flow.

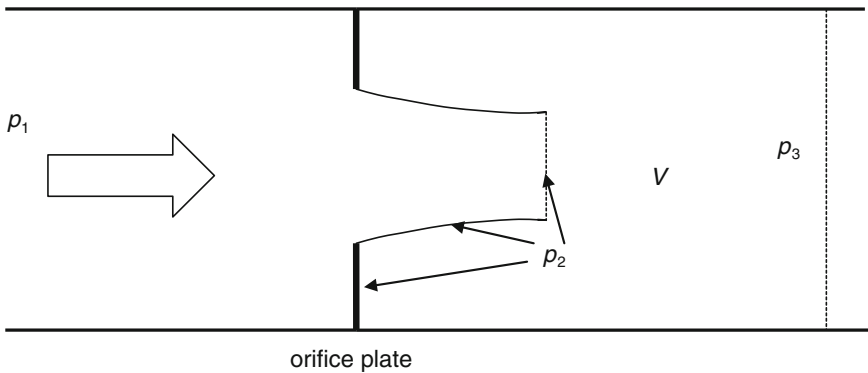


**Fig. 2.20** Pressures during flow through an orifice plate

Then, assuming that the pressure has the same value on the back of the orifice plate, on the edge of the orifice jet as far as the *vena contracta* (i.e. the point of maximum convergence) and at the *vena contracta*, and using the divergence theorem

$$0 = \rho A_c \bar{u}_c^2 - \rho A_p \bar{u}_p^2 - p_3 A_p + p_2 A_p \quad (2.8)$$

where  $A_c$  and  $A_p$  are the area of the *vena contracta* and of the pipe, respectively,  $\bar{u}_c$  and  $\bar{u}_p$  are the mean velocity in the *vena contracta* and in the pipe, respectively, and  $p_2$  and  $p_3$  are the pressure immediately downstream of the orifice (e.g. at a downstream pressure tapping) and after pressure recovery, respectively.

In addition Bernoulli's Equation (see Sect. 1.3) applies between an appropriate location upstream of the orifice plate and the *vena contracta*:

$$p_1 + \frac{1}{2} \rho \bar{u}_p^2 = p_2 + \frac{1}{2} \rho \bar{u}_c^2 \quad (2.9)$$

where  $p_1$  is the pressure around  $1D$  upstream of the orifice.

The basic equation for differential-pressure meters (Eq. 1.15, for incompressible flow) can be expressed as:

$$\bar{u}_o = \frac{C}{\sqrt{1 - \beta^4}} \sqrt{\frac{2(p_1 - p_2)}{\rho}} \quad (2.10)$$

where  $\bar{u}_o$  is the mean velocity in the orifice. Mass conservation between upstream of the orifice plate, the orifice and the *vena contracta* gives:

$$\rho \bar{u}_p A_p = \rho \bar{u}_o \beta^2 A_p = \rho \bar{u}_c A_c. \quad (2.11)$$

Equations 2.8–2.11 give

$$\frac{\Delta \varpi}{\Delta p} = \frac{p_1 - p_3}{p_1 - p_2} = \frac{\sqrt{1 - \beta^4(1 - C^2)} - C\beta^2}{\sqrt{1 - \beta^4(1 - C^2)} + C\beta^2}, \quad (2.12)$$

where  $\Delta \varpi$  is the pressure loss (from  $D$  upstream to  $6D$  downstream).

Of the three standard tapping pairs  $D$  and  $D/2$  tapplings are the most suitable for determining  $C$  for use in Eq. 2.12.

Equation 2.12 is given as Eq. (7) in 5.4.1 of ISO 5167-2:2003. The inclusion of this equation in ISO 5167 resulted from the publication of Urner (1997).

A simpler but less accurate approximation is

$$\frac{\Delta \varpi}{\Delta p} = 1 - \beta^{1.9}, \quad (2.13)$$

which is given in 5.4.2 of ISO 5167-2:2003.

Equation 2.12 has been checked by looking at data from Steven et al. (2007). Strictly speaking Eq. 2.12 is applicable to the situation where the upstream tapping is at  $D$  upstream. Since Steven's tappings were in the flanges his measured pressure loss ratio  $\frac{\Delta\sigma_{up}}{\Delta p_{up}}$  was not equal to the true pressure loss ratio  $\frac{\Delta\sigma}{\Delta p}$ .

The measured pressure loss ratio  $\frac{\Delta\sigma_{up}}{\Delta p_{up}}$ , where the upstream tapping is a flange or a corner tapping, is related to the true pressure loss ratio  $\frac{\Delta\sigma}{\Delta p}$  by

$$\frac{\Delta\sigma_{up}}{\Delta p_{up}} = \frac{p_{up} - p_3}{p_{up} - p_2} = \frac{\frac{\Delta\sigma}{\Delta p} + \frac{p_{up} - p_1}{p_1 - p_2}}{1 + \frac{p_{up} - p_1}{p_1 - p_2}} \quad (2.14)$$

where  $p_{up}$  is the pressure at the upstream pressure tapping. It is not easy, given the assumptions in the use of the momentum theorem, to include a term for the location of the downstream flow-measurement tapping: its effect is small and neglected in Eq. 2.14.

Moreover, from Eq. 1.15,

$$p_{up} \approx p_1 + 2 \frac{C_{D-D/2} - C_{up-D/2}}{C_{D-D/2}} (p_1 - p_2) \quad (2.15)$$

where the difference in discharge coefficient between that for a plate with tappings  $D$  upstream and  $D/2$  downstream,  $C_{D-D/2}$ , and that for a plate with tappings at a different upstream location and  $D/2$  downstream,  $C_{up-D/2}$ , can be obtained from the Reader-Harris/Gallagher (1998) Equation (see Eq. 5.22).

So,

$$\frac{p_{up} - p_1}{p_1 - p_2} \approx 2 \frac{C_{D-D/2} - C_{up-D/2}}{C_{D-D/2}} \quad (2.16)$$

Then the measured pressure loss ratio in Steven et al. (2007) can be compared with calculated values of the pressure loss ratio, obtained by substituting Eqs. 2.12 and 2.16 into Eq. 2.14: see Fig. 2.21. The equation in 2.4.5.1 of API MPMS 14.3.2:2000 is also shown.

It appears possible to predict pressure loss remarkably accurately, but the population of data is very small.

The formula for pressure loss applies where the downstream pressure loss tapping is about  $6D$  downstream of the orifice plate, where the pressure has recovered (to the maximum extent that it does recover). No term for friction loss has been included: it might be appropriate to include one, but, where the upstream and downstream tappings are  $1D$  and  $6D$  respectively from the orifice plate, the friction loss will be significantly less than the friction loss in fully developed flow through  $7D$  of straight pipe.



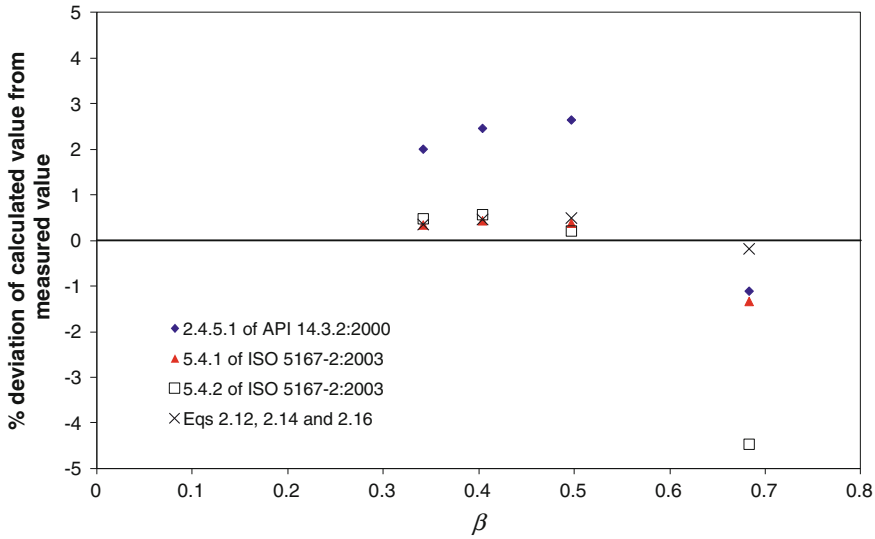


**Fig. 2.21** Pressure loss ratio: deviation of calculated values from measured CEESI data (taken in dry gas for their wet-gas JIP): only ‘Eqs. 2.12, 2.14 and 2.16’ takes specific account of the upstream tapping location

In conclusion, Eq. (7) in ISO 5167-2:2003 for pressure loss ratio (Eq. 2.12) appears remarkably accurate: if the upstream tapping is not located  $1D$  upstream of the orifice plate and the pressure loss ratio that will actually be measured is required, the necessary additional term has been derived.

## 2.7 Reversed Orifice Plates

The effect of reversing an orifice plate is very large. An increase in discharge coefficient of the order of 15 or 20 % is typical. Much of the published literature relating to the discharge coefficients of reversed orifice plates has notable deficiencies when considered for general application. In most papers the orifice plates are not fully described: some papers do not give the bevel angle, and the size of the bevel is rarely stated.

8.6.2 of ISO/TR 12767:2007 (ISO 2007c) provides information on the variation of discharge coefficient with bevel size. However, as no orifice diameter is given, the data cannot be used to determine the magnitude of error in a specific case of interest. 6.1 of ISO/TR 15377:2007 (ISO 2007b) describes the ‘conical entrance’ orifice, which is considered to have a constant discharge coefficient of 0.734. However, the conical entrance orifice is not sufficiently representative of reversed square-edged orifice plates to give results of general application. In SPE Note 22867 (Ting 1991) the author describes the results of a number of tests with air at

low Reynolds numbers. The tests were carried out for various  $\beta$ , but neither bevel angle nor bevel size is given in the paper. When consulted, the author stated that he believed that the bevel angle was  $30^\circ$  to the face of the plate.

Witte (1997) published a paper on the effect of reversing orifice plates in a 10" pipe in gas at 60 barg. The plates had thickness,  $E$ , of 6.35 mm ( $1/4$ " ) with  $45^\circ$  bevel. The orifice (bore) thickness,  $e$ , was 4.76 mm ( $3/16$ " ), although this is not stated in the paper. Witte carried out the work at the Gas Research Institute Metering Research Facility at Southwest Research Institute. Morrow (2000) reanalysed Witte's data. CFD was undertaken by Brown et al. (2000). Morrow also measured the effect of reversing a series of plates in a 4" line; these plates had a bevel angle of  $45^\circ$ , a plate thickness,  $E$ , of 3.18 mm ( $1/8$ " ) and an orifice (bore) thickness,  $e$ , of 1.59 mm ( $1/16$ " ). George and Morrow presented the data listed above and both 2" data and additional 4" data and presented conclusions in George and Morrow (2001).

Even where the bevel angle is  $45^\circ$  no simple formula has achieved universal acceptance. The correlation in George and Morrow (2001), also quoted in Morrow et al. (2002), is

$$\% \text{flowrate error} = -18.93 + 12.91\beta - 34.04 \frac{E}{D_{nom}} - 8.900 \frac{e}{E} + 13.64 \left( \frac{e}{E} \right)^2 \quad (2.17)$$

This does not have the correct performance in the limit as  $b/E$  tends to 0, where  $b$  is the bevel width ( $=E - e$ ), (i.e.  $e/E$  tends to 1).

The error should be a function of  $b/d$  (similar to edge rounding), but not of  $b/d$  alone:  $\beta$  is significant too. Figure 2.22 shows the experimental data for bevel angle  $45^\circ$  from SwRI including those of Witte plus two points from NEL. The lines described as 'experiment' join up the experimental data for each value of  $\beta$ . If the bevel is treated as a rounded edge and the best-fit radius determined as in Sect. 2.2.4, then the best-fit radius is  $1.57b$  (presumably  $\pi b/2$ ). Then the expected flowrate error for a bevelled edge can be calculated as in Sect. 2.2.4. This has been plotted for a maximum ratio of edge radius to diameter of 0.01, since the data of Burgin (1971) show that above that value the data deviate increasingly from the fit in Sect. 2.2.4.

The data from Witte appear different (especially for  $\beta = 0.2$ ) from the other data sets. This could be due to  $e/E$  being equal to 0.75. So the other data points (i.e. those for  $e/E \leq 0.5$ ) in Fig. 2.22 were fitted with the following equation:

$$\% \text{flowrate error} = -(a - b\beta^c) \left( 1 - \exp \left( \frac{-f \frac{b}{d}}{a - b\beta^c} \right) \right)$$

This behaves correctly as  $b/d$  tends to 0.

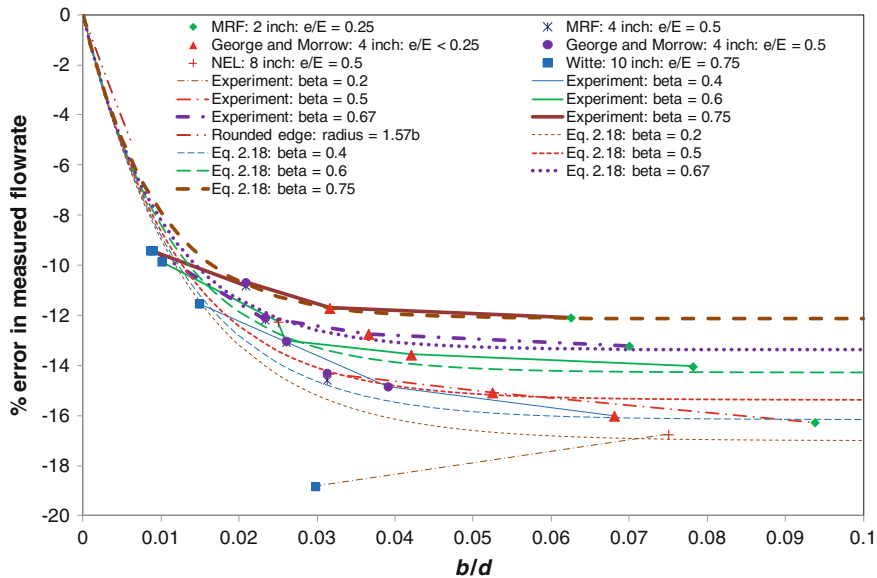


Fig. 2.22 Error in measured flowrate using a reversed orifice plate

With the fit

$$\%flowrate\ error = -(17.2 - 10.4\beta^{2.5}) \left( 1 - \exp\left(\frac{-1270\frac{b}{d}}{17.2 - 10.4\beta^{2.5}}\right) \right) \quad (2.18)$$

the r.m.s. deviation of the equation from the data is 0.35 %. Equation 2.18 is shown on Fig. 2.22.

To avoid having a problem with a reversed plate, where possible a plate should be marked externally in such a way that correct orientation can be verified without looking into the pipe.

## 2.8 Conclusions

This chapter has described the main design specifications for orifice plates: it has pointed the reader to important parts of ISO 5167 and given reasons for the requirements in the standard. It has covered the orifice plate (the circularity of the bore, the flatness, the parallelism of the two faces, the surface condition of the upstream face, and, above all, the edge sharpness), the pipe (the pressure tapings, the pipe roughness, the effect of upstream steps, the concentricity of the orifice plate in the pipe and the circularity and cylindricity of the pipe), the measurements of both the orifice plate and the pipe, and the pressure loss. A very significant incorrect installation of an orifice plate within the pipe, a reversed orifice plate, has also been

covered. Appendix 2.A considers the use of orifice plates of diameter smaller than that permitted in ISO 5167-2:2003.

The basic instruction remains to follow ISO 5167. For some important deviations from ISO 5167 the errors in discharge coefficient can be calculated using what is described in this chapter.

## Appendix 2.A: Orifice Plates of Small Orifice Diameter

### 2.A.1 Introduction and Test Work

Orifice plates of small orifice diameter,  $d$ , are often used for measuring low gas flowrates in declining wells in order to increase the available differential pressure. However, some flowrates may result in the orifice diameter being sufficiently small that the orifice diameter is outside ISO 5167-2:2003, i.e. less than 12.5 mm (0.492").

Twelve orifice plates were obtained and tested by NEL for ConocoPhillips, four of them from a manufacturer that specializes in spark erosion techniques, eight of them from a manufacturer that specializes in orifice plates. The aim was to determine the probable errors that might be obtained in using orifice plates of very small sizes.

Accordingly four orifice plates were manufactured for the project by ATM (Advanced Tool Manufacture), East Kilbride, Scotland and used electrical discharge machining (EDM—or spark erosion) to machine the orifice bore; eight were manufactured by Kelley Orifice Plates, Texarkana, Texas using conventional machining techniques. From ATM, the orifice diameters were 6.35 mm ( $1/4"$ ), 3.18 mm ( $1/8"$ ) (2 off) and 1.59 mm ( $1/16"$ ); from Kelley they were 9.52 mm ( $3/8"$ ), 6.35 mm ( $1/4"$ ), 3.18 mm ( $1/8"$ ) and 1.59 mm ( $1/16"$ ) (2 off in each case). In the case of ATM  $e/d = 0.1$  was specified, where  $e$  is the thickness of the orifice, and  $d$  the orifice diameter (see Sect. 2.2.5).

All the orifice plates were calibrated in water in a 4" line ( $D = 101.80$  mm) over a range of Reynolds number. The Reynolds number was below the minimum pipe Reynolds number of 5000 permitted by ISO 5167-2:2003 for all the data, except for most of the  $d = 9.52$  mm ( $3/8"$ ) data. The data are shown in Reader-Harris et al. (2008). The smallest value of pipe Reynolds number was 116; so the deviations here are presented from the complete orifice plate discharge-coefficient equation:

$$\begin{aligned}
C = & 0.5961 + 0.0261\beta^2 - 0.216\beta^8 + 0.000521 (10^6\beta/Re_D)^{0.7} \\
& + (0.0188 + 0.0063A)\beta^{3.5}\max\{(10^6/Re_D)^{0.3}, 22.7 - 4700 (Re_D/10^6)\} \\
& + (0.043 + 0.080 e^{-10L_1} - 0.123 e^{-7L_1})(1 - 0.11A) \frac{\beta^4}{1 - \beta^4} \\
& - 0.031 (M'_2 - 0.8M_2'^{1.1})\{1 + 8\max(\lg(3700/Re_D), 0.0)\}\beta^{1.3} \\
& + 0.011 (0.75 - \beta)\max(2.8 - D/25.4, 0.0)
\end{aligned} \tag{5.21}$$

where  $D$  is the pipe diameter in mm (following ISO 80000-2:2009,  $\log_{10}$  is written  $\lg$ ).

The Reader-Harris/Gallagher (1998) Equation in ISO 5167-2:2003 (ISO 2003b) (given here as Eq. 5.22) is the special case of Eq. 5.21 for  $Re_D \geq 5000$ . The differences between Eq. 5.21 and the extrapolated Reader-Harris/Gallagher (1998) Equation are very small, less than 0.06 % in magnitude, over the range of the data here.

For each orifice plate the mean deviation of the data from Eq. 5.21 over its range of Reynolds number is given in Fig. 2.A.1: the mean deviations are plotted against orifice diameter. To use a simple additive correction to Eq. 5.21 for each orifice plate it is necessary that the deviation be almost constant over its range of Reynolds number: for each orifice plate the standard deviation of the deviations from Eq. 5.21 over its range of Reynolds number is given in Fig. 2.A.2.

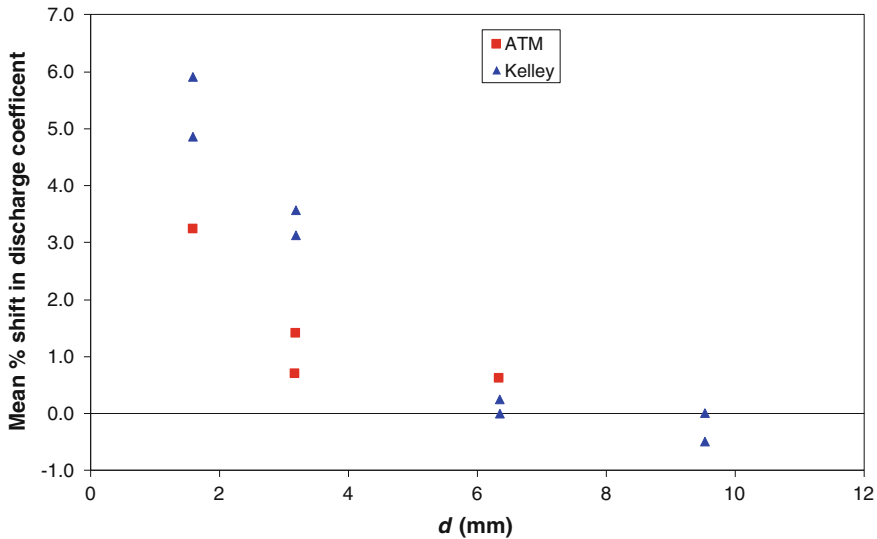


**Fig. 2.A.1** Mean percentage shift in discharge coefficient from Eq. 5.21 for each orifice plate over its range of Reynolds number

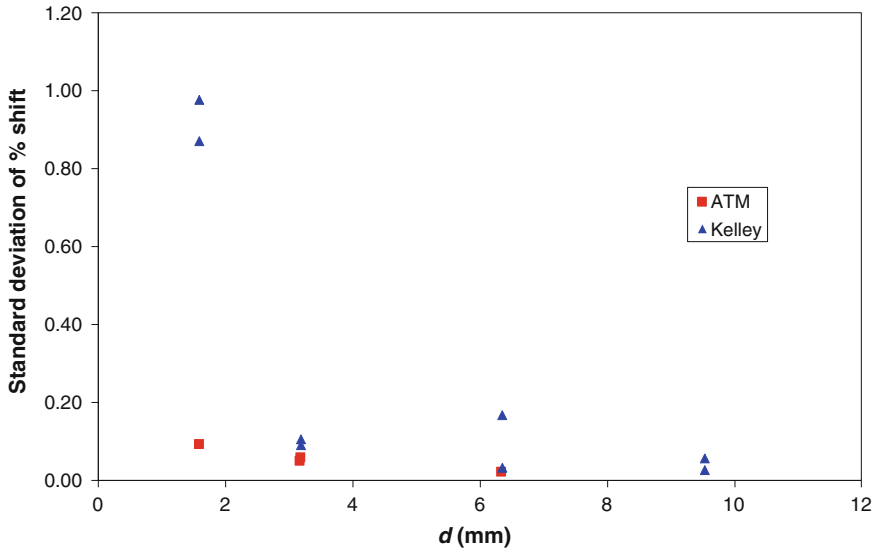


**Fig. 2.A.2** Standard deviation of percentage shift in discharge coefficient from Eq. 5.21 for each orifice plate over its range of Reynolds number

From Fig. 2.A.2 for all the ATM data and for most of the Kelley data the deviation from Eq. 5.21 (and hence from the Reader-Harris/Gallagher (1998) Equation) was fairly constant and so Eq. 5.21 could be used with a simple additive correction, presumably due to edge rounding. The fact that there appears to be a simple rounding correction for most of the sets supports the view that, given such an edge-rounding term, Eq. 5.21 can be used with general success for orifice plates that have both small  $d$  and small  $\beta$ .

If the orifice plates calibrated here were to be used in service they would be used with a simple additive shift as given in Fig. 2.A.1. Since, however, they were a sample of plates used to determine how other plates from the same manufacturers would perform in service then further analysis was necessary.

If the edge radius of an orifice plate is  $r$ , and the increase in edge radius is  $\Delta r$ , the percentage increase in discharge coefficient,  $S$ , is given by Hobbs and Humphreys (1990) (see Sect. 2.2.4):

$$S = 550 \frac{\Delta r}{d}. \quad (2.A.1)$$

So given a shift in discharge coefficient it is possible to calculate the increase in edge radius that gives rise to it. It is not clear on what relative edge radius Eq. 5.21 is based at the low throat Reynolds numbers obtained with these plates. If it were

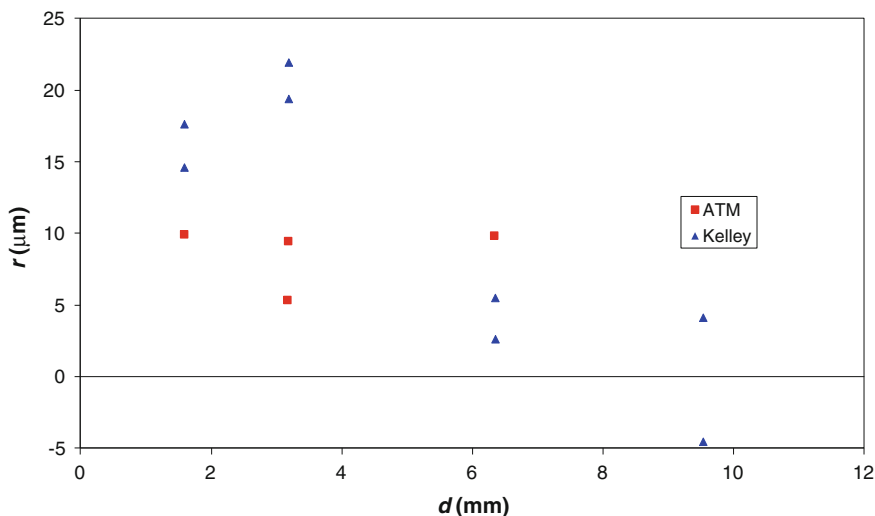


**Fig. 2.A.3** Calculated edge radius of orifice plates v  $d$

assumed that it is based on  $r/d = 0.0004$ , that is the maximum permitted edge radius in ISO 5167-2:2003 (at high Reynolds numbers with larger plates Eq. 5.21 (and thus the Reader-Harris/Gallagher (1998) Equation) is based on relatively sharper plates), then the edge radii for the different plates would be as shown in Fig. 2.A.3.

The mean edge radius of the ATM plates is calculated to be 8.7 μm.

NOTE If the PR 14 Equation (Eq. 5.C.2) were used instead of Eq. 5.21 the mean edge radius of the ATM plates would be calculated to be 10.9 μm. If Eq. 5.21 were used but it were assumed that at these low throat Reynolds numbers Eq. 5.21 was based on  $r/d = 0.0003$  the mean edge radius of the ATM plates would be calculated to be 0.36 μm smaller than if Eq. 5.21 were based on  $r/d = 0.0004$ .

When the following term (based on an edge radius of 8.7 μm and Eq. 2.A.1) is used

$$\Delta C = 3.3 \left( \frac{0.0087}{d} - 0.0004 \right) (d : \text{mm}) \quad (2.A.2)$$

95 % of the ATM data lie within 0.65 % of Eq. 5.21 with term 2.A.2 added.

In Fig. 2.A.4 the data from the spark-eroded plates are compared with Eq. 5.21 (essentially the Reader-Harris/Gallagher (1998) Equation) with an additional term representing an edge radius of 8.7 μm.

The Stolz Equation in ISO 5167:1980 (ISO 1980) (given here as Eq. 5.24) does not give good performance as  $\beta$  tends to 0.

It is more difficult to analyse the data from the Kelley plates: the analysis is provided in Reader-Harris et al. (2008).

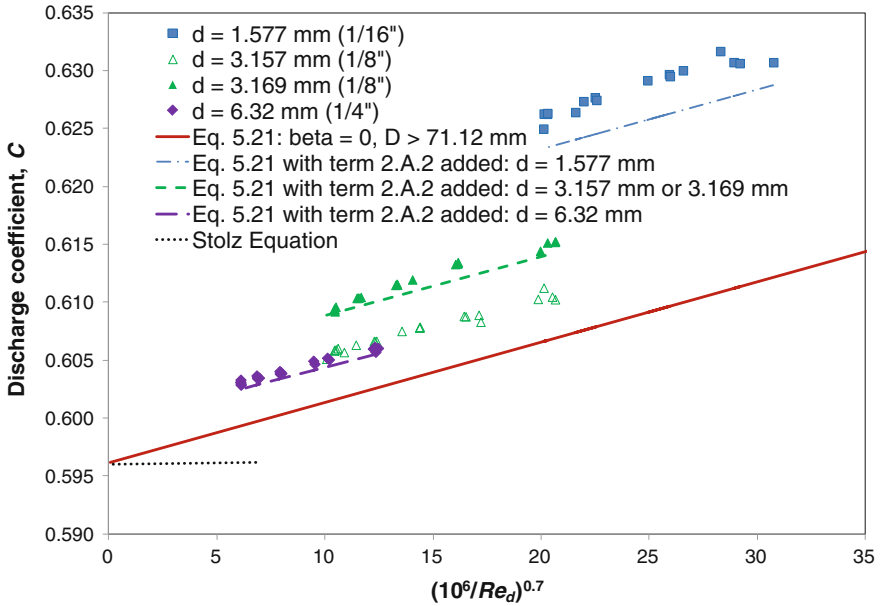


Fig. 2.A.4 The discharge-coefficient data from the spark-eroded orifice plates

## 2.A.2 Conclusions

Orifice plates can be a surprisingly good way of measuring small gas flows. The Reader-Harris/Gallagher Equation appears to work well for small orifices if an additional term is added to allow for edge rounding (from Sect. 2.2.5 it would be wise also to specify that  $e/d \leq 0.1$ ). The edge radius for the spark-eroded plates appears to be fairly constant as  $d$  decreases, and so for uncalibrated spark-eroded orifice plates from one manufacturer good results may be obtained by adding term 2.A.2 arithmetically to the Reader-Harris/Gallagher (1998) Equation. Results presumably depend on the manufacturer. An orifice plate with edge radius equal to the average edge radius of the plates manufactured by ATM will meet the requirements of ISO 5167-2:2003 provided that  $d$  is greater than 22 mm. On this basis in a 24" line an orifice plate with  $\beta = 0.05$  would still have a sharp edge and not require an additional term added to the discharge-coefficient equation.

To be able to use orifice plates of very small orifice diameter in an existing installation in a declining gas field may be much more economical than to replace the metering or shut the field. From the beginning of the flow measurement to its conclusion a 4" orifice meter with different orifice plates (including those described in this appendix) might measure a range of around 3000:1 in terms of mass flowrate (if the static pressure were the same throughout the period of measurement).



## References

- AGA (1951) Investigation of orifice meter installation requirements. American Gas Association
- AGA (1954a) Investigation of orifice meter installation requirements. American Gas Association
- AGA (1954b) Large diameter orifice meter tube tests. Final report of Supervising Committee. Research Project NX-4. American Gas Association
- API (2000) Natural Gas Fluids Measurement. Part 2—Specification and Installation Requirements—Concentric, Square-edged Orifice Meters. API MPMS (Manual of Petroleum Measurement Standards) Chapter 14.3.2:2000. American Petroleum Institute, Washington, DC
- Barton N, Hodgkinson E, Reader-Harris MJ (2005) Estimation of the measurement error of eccentrically installed orifice plates. In: Proc 23rd North Sea Flow Meas Workshop, Norway: Paper 4
- Bean HS, Murdock JW (1959) Effects of pipe roughness on orifice meter accuracy, Report of Supervising Committee on two-inch tests. American Gas Association Research Project NW-20, American Gas Association, New York
- Beitler SR (1935) The flow of water through orifices. A study in 1-in., 1½-in., 2-in., 3-in., 6-in., 10-in, and 14-in. lines. Engineering Experiment Station Bulletin No 89. Ohio State University
- Benedict RP, Wyler JS, Brandt GB (1974) The effect of edge sharpness on the discharge coefficient of an orifice. Trans ASME J. Eng. Power: paper No 74-WA/FM-4
- Botros KK, Studzinski W, Barg P (1992) Results of NOVA's gas metering research. Canadian Gas Association, Measurement School, Vancouver, May 26–29
- Brain TJS, Reid J (1973) Measurement of orifice plate edge sharpness. Meas Control 6:377–384
- Brennan JA, McFaddin SE, Sindt CF, Wilson RR (1989) Effect of pipe roughness on orifice flow measurement. NIST Technical Note 1329. National Institute of Standards and Technology, Boulder, Colorado
- Brown GJ, Reader-Harris MJ, Gibson JJ, Stobie GJ (2000) Correction of readings from an orifice plate installed in reverse orientation. In: Proceedings of 18th North Sea Flow Meas Workshop, Gleneagles: Paper 2.2. National Engineering Laboratory, East Kilbride, Glasgow
- Burgin EJ (1971) Factors affecting accuracy of orifice measurement (primary element). In: Proceedings of International School Hydrocarbon Measurement
- Clark WJ, Stephens RC (1957) Flow measurement by square edged orifice plates: pipe roughness effects. Inst Mech Eng 171(33):895–904
- Crocket KA, Upp EL (1973) The measurement and effects of edge sharpness on the flow coefficients of standard orifices. Trans ASME J Fluids Eng (June): 271–275 (also paper No 72-WA/FM-4, 1972)
- Dall HE (1958) The effect of roughness of the orifice plate on the discharge coefficient. Instrument Engineer: 2(5) (April)
- Gallagher GR (1968) Measuring edge sharpness of orifice plates. The Engineer, 17 May 1968
- George DL, Morrow TB (2001) Orifice meter calibration for backwards-facing orifice plates. GRI Report No 01/0074 on SwRI Project No 18-8890. Gas Research Institute, Chicago
- Goodson FD, Zanker K, Husain ZD (2004) The effects of upstream recesses on the discharge coefficient of a flange tapped orifice meter. AGA Operations Conference
- Gorter J (1978) Deformation of orifice plates: theory and practice. In: Dijkstra HH, Spencer EA (eds) Flow measurement of fluids. North-Holland Publishing Company
- Herning F (1962) Untersuchungen zum Problem der Kantenunschärfe bei Normblenden und bei Segmentblenden [Experiments on the problem of the edge sharpness of standard and segmental orifice plates]. Brennst-Wärme-Kraft 14(3):119–126
- Herning F, Lugt H (1958) Neue Versuche mit Segmentblenden und Normblenden. Brennst-Wärme-Kraft 10(5):219–223
- Herning F, Wolowski E (1963) Die Kantenunschärfe von Normblenden und Segmentblenden und das Ähnlichkeitsgesetz [The edge sharpness of standard and segment orifices and the laws of similarity]. Brennst-Wärme-Kraft 15(1):26–30

- Hobbs JM, Humphreys JS (1990) The effect of orifice plate geometry upon discharge coefficient. *Flow Meas Instrum* 1(3):133–140
- Husain ZD, Goodson FD (1986) Effects of plate thickness and bevel angle on discharge coefficients of a 50 mm (2 inch) orifice meter. ASME paper 86-WA/FM-4, Winter Annual Meeting, FM-4 Symposium on Flowmeters, Anaheim, California, December 1986
- Husain ZD, Teyssandier RG (1986a) Orifice eccentricity effects for flange, pipe and radius (D-D/2) taps. ASME paper 86-WA/FM-1, presented at ASME Winter Annual Meeting, Anaheim, California
- Husain ZD, Teyssandier RG (1986b) The effects of plate thickness and bevel angle in a 150 mm line size orifice meter. In: *Proceedings of flow measurement in the mid 80s*. National Engineering Laboratory, East Kilbride, Glasgow
- ISO (1980) Measurement of fluid flow by means of orifice plates, nozzles and Venturi tubes inserted in circular cross-section conduits running full. ISO 5167:1980. International Organization for Standardization, Geneva
- ISO (1991) Measurement of fluid flow by means of pressure differential devices—Part 1: orifice plates, nozzles and Venturi tubes inserted in circular cross-section conduits running full. ISO 5167-1:1991. International Organization for Standardization, Geneva
- ISO (2003a) Measurement of fluid flow by means of pressure differential devices inserted in circular cross-section conduits running full—Part 1: general principles and requirements. International Organization for Standardization, Geneva. ISO 5167-1:2003
- ISO (2003b) Measurement of fluid flow by means of pressure differential devices inserted in circular cross-section conduits running full—Part 2: Orifice plates. Geneva: International Organization for Standardization. ISO 5167-2:2003
- ISO (2007a) Fluid flow in closed conduits—Connections for pressure signal transmissions between primary and secondary elements. International Organization for Standardization, Geneva. ISO 2186:2007
- ISO (2007b) Measurement of fluid flow by means of pressure differential devices—Guidelines for the specification of orifice plates, nozzles and Venturi tubes beyond the scope of ISO 5167. International Organization for Standardization, Geneva. ISO/TR 15377:2007
- ISO (2007c) Measurement of fluid flow by means of pressure differential devices—Guidelines on the effect of departure from the specifications and operating conditions given in ISO 5167. International Organization for Standardization, Geneva. ISO/TR 12767:2007
- ISO (2008) Guidelines for the use of ISO 5167:2003. International Organization for Standardization, Geneva. ISO/TR 9464:2008
- Jepson P, Chipchase R (1973) The effect of plate buckling on orifice meter accuracy. Report No ERS.R.467, British Gas Engineering Research Station
- Jepson P, Chipchase R (1975) Effect of plate buckling on orifice meter accuracy. *J Mech Eng Sci* 17(6):330–337
- Johansen WR (1966) Effects of thin films of liquid coating orifice plate surfaces on orifice flowmeter performance. GRI Report No GRI-96/0375. Gas Research Institute, Chicago
- Johansen W, Seidl W, Kegel T (1966) The effects of oil coating on the measurement of gas flow using sharp-edged orifice flowmeters. American Gas Association: AGA Operating section Conference, Montreal
- Lansverk NB (1990) Effects of abnormal conditions on accuracy of orifice measurement. ISHM. (sent by Loy Upp)
- Mason D, Wilson MP, Birkhead WG (1975) Measurement error due to the bending of orifice plates. ASME Winter Annual Meeting, Houston, Texas: Paper 75-WA/FM-6. American Society of Mechanical Engineers
- McVeigh JC (1962) Further investigations into the effect of roughness of the orifice plate on the discharge coefficient. *Instrument Engineer*, pp 112–113
- Miller RW, Kneisel O (1968) Experimental study of the effects of orifice plate eccentricity on flow coefficients. *ASME J Basic Eng*, pp 12–131, March 1969, previously presented at ASME Winter Annual Meeting, New York, December 1–5, Paper 68-WA/FM-1, 1968

- Morrison GL, DeOtte RE, Moen M, Hall KR, Holste JC (1990) Beta ratio, swirl and Reynolds number dependence of wall pressure in orifice flowmeters. *Flow Meas Instrum* 1:269–277
- Morrow TB (1998) Effects of oil on orifice plates in gas flow measurement. In: *Proc ASME Fluids Eng. Div. Summer Meeting*, paper FEDSM98-M284. American Society of Mechanical Engineers, Washington, DC
- Morrow TB (2000) Private communication. GRI MRF, San Antonio, Texas
- Morrow TB, Morrison GL (1999) Effect of meter tube roughness on orifice  $C_d$ . In: 4th international symposium on fluid flow meas, Denver
- Morrow TB, George DL, Nored MG (2002) Operational factors that affect orifice meter accuracy. MRF Topical Report GRI-00/0141 on SwRI Project No 18-8890. Gas Research Institute, Chicago
- Norman R, Rawat MS, Jepson P (1983) Buckling and eccentricity effects on orifice metering accuracy. International Gas Research Conference
- Norman R, Rawat MS, Jepson P (1984) An experimental investigation into the effects of plate eccentricity and elastic deformation on orifice meter accuracy. In: Spencer EA (ed) *Proceedings of International Conference Metering of Natural Gas and Liquefied Hydrocarbon Gases*, London, UK, 1–2 Feb 1984, paper 3.3. Oyez, London
- Pritchard M, Niazi A, Marshall D (2003) Assessment of the effect of contamination on orifice plates. In: *Proceedings of 11th Flomeko conference on flow measurement of gas and liquid*, Groningen, 12–14 May 2003: Paper 6.2. Gasunie Research, Groningen (on CD-ROM)
- Pritchard M, Marshall D, Wilson J (2004) An assessment of the impact of contamination on orifice plate metering accuracy. In: *Proceedings of 22nd North Sea Flow Meas Workshop*, St Andrews: Paper 2.2. National Engineering Laboratory, East Kilbride, Glasgow
- Reader-Harris MJ (1990) Pipe roughness and Reynolds number limits for the orifice plate discharge coefficient equation. In: *Proceedings of 2nd International Symposium Fluid Flow Meas*, Calgary, pp 29–43
- Reader-Harris MJ (1991) The effect of plate roughness on orifice plate discharge coefficients. *Flow Measurement Memo. FL/421*. National Engineering Laboratory Executive Agency, East Kilbride, Glasgow
- Reader-Harris MJ (1993) The effect of plate roughness on orifice plate discharge coefficients—Further work. *Flow Measurement Memo FL/438*. National Engineering Laboratory Executive Agency, East Kilbride, Glasgow
- Reader-Harris MJ, Brunton WC (2002) The effect of diameter steps in upstream pipework on orifice plate discharge coefficients. In: *Proceedings of 5th International Symposium Fluid Flow Meas*, Washington, DC
- Reader-Harris MJ, Keegans W (1986) Comparison of computation and LDV measurement of flow through orifice and perforated plates, and computation of the effect of rough pipework on orifice plates. In: *Proceedings of International Symposium Fluid Flow Meas*, pp 653–666, Washington, DC
- Reader-Harris MJ, Brunton WC, Nicholson IG, Rushworth R (2003) Ageing effects on orifice metering. In: *Proceedings of 21st North Sea Flow Meas Workshop*, Norway
- Reader-Harris MJ, Stobie G, Kelley T (2008) The discharge coefficient of orifice plates with diameters from  $1/16''$  (1.6 mm) to  $3/8''$  (9.5 mm). In: *Proceedings of Production and Upstream Flow Meas Workshop*, Houston, Texas
- Reader-Harris MJ, Barton N, Hodges D (2010) The effect of contaminated orifice plates on the discharge coefficient. In: *Proceedings of 15th FLOMEKO*, Taipei
- Schlichting H (1960) *Boundary layer theory*. McGraw-Hill, New York
- Spencer EA (1987) Study of edge sharpness effects measured during the EEC orifice plate coefficient programme. BCR Report EUR 11131, Commission of the European Communities, Brussels
- Spencer EA, Calame H, Singer J (1969) Edge sharpness and pipe roughness effects on orifice plate discharge coefficients. NEL Report No 427. National Engineering Laboratory, East Kilbride, Glasgow

- Steven R, Britton C, Stewart D (2007) CEESI Wet Gas JIP Data Release. EI/CEESI Wet Gas Metering Seminar Aberdeen. CEESI, Colorado
- Stewart IA (1989) The EEC 600 mm orifice meter project. Part II Inspection of the meter run and orifice plates. Report No ERS.R.4255, British Gas Engineering Research Station
- Studzinski W, Berg D (1988) Effects of orifice surface conditions on accuracy of flow rate measurements. In: Proceedings of 2nd International Conference on Flow Meas, London. BHRA, Cranfield, Bedfordshire
- Studzinski W, Berg D, Bell D, Karwacki L (1990) Effect of meter run roughness on orifice meter accuracy. In: Proceedings of 2nd International Symposium Fluid Flow Meas, Calgary, pp 1–15
- Teyssandier RG (1985) The effect of symmetric steps and gaps on orifice measurement. In: Proceedings of 3rd North Sea Flow Meas Workshop, Norway
- Thibessard G (1960) Le coefficient de débit des diaphragmes, la rugosité et le nombre de Reynolds. *Chaleur et Industrie* 415:33–50
- Ting VC (1991) Effects of non-standard operating conditions on the accuracy of orifice meters. SPE 22867. Society of Petroleum Engineers
- Ting VC, Corpron GP (1995) Effect of liquid entrainment on the accuracy of orifice meters for gas flow measurement. Int Gas Research Conf
- Uerner G (1997) Pressure loss of orifice plates according to ISO 5167-1. *Flow Meas Instrum* 8 (1):39–41
- Whetstone JR, Cleveland WG, Baumgarten GP, Woo S (1989) Measurements of coefficients of discharge for concentric, flange-tapped, square-edged orifice meters in water over a Reynolds number range of 1000–2,700,000. NIST Technical Note TN-1264. NIST, Washington, DC
- Witte R (1953) Neue Beiträge zur internationalen Normung auf dem Gebiete der Durchflußmessung. *Brennst-Wärme-Kraft* 5(6):185–190
- Witte JN (1997) Orifice meter error with reversed beveled plates. In: Proceedings of AGA operating conference, Nashville, Tennessee: paper 97-OP-062
- Zedan MF, Teyssandier RG (1990) Effect of errors in pressure tap locations on the discharge coefficient of a flange-tapped orifice plate. *Flow Meas Instrum* 1(3):141–148

<http://www.springer.com/978-3-319-16879-1>

Orifice Plates and Venturi Tubes

Reader-Harris, M.

2015, XVIII, 393 p. 220 illus., 192 illus. in color.,

Hardcover

ISBN: 978-3-319-16879-1